농학박사 학위논문

세균벼알마름병균 (*Burkholderia glumae*)에서 유전체 구조와 양분 스트레스가 정족수 감지 기반 유전자 조절 돌연변이의 발생에 미치는 영향

Influence of genomic structure and nutrient stress on the occurrence of quorum sensing-dependent gene-regulating mutations in *Burkholderia glumae*

2022년 8월

서울대학교 대학원

농생명공학부 식물미생물학전공

강 민 희

Influence of genomic structure and nutrient stress on the occurrence of quorum sensing-dependent gene-regulating mutations in *Burkholderia glumae*

A dissertation submitted in partial
fulfillment of the requirement for
the degree of

DOCTOR OF PHILOSOPHY

to the Faculty of
Department of Agricultural Biotechnology
at

SEOUL NATIONAL UNIVERSITY

by

Minhee Kang

AUGUST 2022

농학박사 학위논문

세균벼알마름병균 (*Burkholderia glumae*)에서 유전체 구조와 양분 스트레스가 정족수 감지 기반 유전자 조절 돌연변이의 발생에 미치는 영향

지도교수 손 호 경

이 논문을 농학박사 학위논문으로 제출함
2022년 7월

서울대학교 대학원
농생명공학부 식물미생물학전공

강 민 희

강민희의 박사 학위논문을 인준함

2022년 7월

위 원 장 김 국 형 (인)

부 위 원 장 손 호 경 (인)

위 원 김 광 형 (인)

위 원 이 제 훈 (인)

위 원 이 정 관 (인)

A THESIS FOR THE DEGREE OF DOCTOR OF PHILOSOPHY

Influence of genomic structure and nutrient stress on the occurrence of quorum sensing-dependent gene-regulating mutations in *Burkholderia glumae*

UNDER THE DIRECTION OF DR. HOKYOUNG SON

SUBMITTED TO THE FACULTY OF THE GRADUATE SCHOOL
OF SEOUL NATIONAL UNIVERSITY

BY
MINHEE KANG

PROGRAM IN PLANT MICROBIOLOGY
DEPARTMENT OF AGRICULTURAL BIOTECHNOLOGY

JULY 2022

APPROVED AS A QUALIFIED THESIS OF MINHEE KANG
FOR THE DEGREE OF DOCTOR OF PHILOSOPHY
BY THE COMMITTEE MEMBERS

CHAIRMAN	Kook-Hyung Kim
VICE CHAIRMAN	Hokyoung Son
MEMBER	Kwang-Hyung Kim
MEMBER	Jae Hoon Lee
MEMBER	Jungkwan Lee

ABSTRACT

Influence of genomic structure and nutrient stress on the occurrence of quorum sensing-dependent gene-regulating mutations in *Burkholderia glumae*

Minhee Kang
Program in Plant Microbiology
Department of Agricultural Biotechnology
The Graduate School
Seoul National University

Bacteria often alter their genetic and physiological traits to adapt in barren environments. *Burkholderia glumae* is a plant pathogen that has a wide range of hosts, including rice and Solanaceous crops, causing bacteria wilt and rice panicle blight. This bacterium is characterized by high versatility and adaptability to various ecological niches. In order to confirm whether the genomic diversity in *B. glumae* is related to the ability to adapt to ever-changing environment, we performed whole genome analysis on 44 isolates from various regions and sources. All isolates classified into six clusters and two divisions via whole-genome phylogenetic analysis. All isolates except for BGR80S and BGR81S, which had two chromosomes combined

into one, possessed two chromosomes. By comparing genomic structures of *B. glumae* isolates to the prototype BGR1, there were inversions, deletions, and rearrangements within or between chromosomes 1 and/or 2. When BGR80S, BGR15S, and BGR21S, corresponding to clusters III, IV, and VI, were grown in Luria-Bertani medium, spontaneous null mutations occurred in *qsmR* encoding a quorum-sensing master regulator. *qsmR* mutants were observed at detectable frequencies in BGR15S and BGR21S from the 6th day of subculture, and reached approximately 40% at 8 days after subculture. However, *qsmR* mutants were first observed 2 days after subculture in BGR80S and reached almost 80%. No *qsmR* mutant was detected at detectable frequency in BGR1 or BGR13S. When the spontaneous *qsmR* mutants were co-cultured with their parental strains, mutants were outcompeted in their growth. As glucose or casamino acids were added daily to the batch cultures of BGR80S, the emergence of *qsmR* mutants was delayed and their incidence was significantly reduced. These results demonstrate that the occurrence of spontaneous *qsmR* mutations is associated with genomic structure and nutrient stress.

Keywords: *Burkholderia glumae*, genome variation, QsmR mutant, adaptation

Student number: 2015-23124

CONTENTS

LIST OF TABLES

LIST OF FIGURES

Influence of genomic structural variations and nutritional conditions on the emergence of quorum sensing-dependent gene regulation defects in *Burkholderia glumae*

This chapter was published in Frontiers in Microbiology

Kang, M., Lim, J.Y., Kim, J., Hwang, I., Goo, E. (2022).

doi: 10.3389/fmicb.2022.950600

INTRODUCTION

In natural microbial populations, physiologically or genetically distinct variants often exist, having evolved by adapting to the environmental conditions of their natural habitat (Achtman and Wagner, 2008). Closed batch cultures provide an excellent, easy to use laboratory system for studying adaptive variants to nutrient stress, because bacterial cells can be cultured for several days without the addition of nutrients (Ratib et al., 2021). The relative fitness benefits of these variants, and their strategies for adapting to various stresses, have been studied in different microorganisms (Helsen et al., 2020; Aggeli et al., 2021).

In this study, comparative genome analysis and experiments were performed targeting *Burkholderia glumae*. *Burkholderia glumae* has a wide range of hosts, including rice, tomato, pepper, and potato, causing rice panicle blight and bacterial wilt (Jeong et al., 2003). Although *B. glumae* is known as a plant pathogen, the clinical isolate *B. glumae* strain AU6208 has been reported from patients with chronic infections (Weinberg et al., 2007). The sequenced genomes of plant-associated *B. glumae* strains, including 336gr-1, LMG2196, and PG1, and the clinical isolate AU6208, were compared with that of *B. glumae* BGR1 isolated from an infected rice plant in South Korea (Francis et al., 2013; Lee et al., 2016; Hussain et al., 2020). These comparative studies revealed that while the isolates share common characteristics, such as toxoflavin biosynthesis genes, unique genomic regions and large-scale genome rearrangement and inversion were observed in each strain (Francis et al., 2013; Lee et al., 2016; Hussain et al., 2020). However, whether

the genotypically distinct isolates of *B. glumae* have distinctive physiological traits and evolutionary routes for environmental adaptation is unknown.

B. glumae has a single LuxIR-type TofIR quorum sensing (QS) system that regulates the biosynthesis of toxoflavin, a key virulence factor, and activates the expression of the IclR-type transcription regulator *qsmR* (Kim et al., 2004; Kim et al., 2007). QsmR regulates the expression of dozens of genes, including flagella and oxalate biosynthesis genes, in a TofIR-dependent manner (Kim et al., 2007; Goo et al., 2012). When *B. glumae* is cultured in Luria-Bertani (Pesci et al.) medium, ammonia accumulates due to deamination using amino acids as a carbon source (Goo et al., 2012). To neutralize the alkaline toxicity mediated by ammonia, oxalate is biosynthesized in a QsmR-dependent manner (Goo et al., 2012). These results allowed us to investigate how QS-dependent physiological traits differ among *B. glumae* isolates originating from different hosts and regions.

Previously, comparative genomic analysis studies of *Burkholeria* interspecies or intraspecies existed, but there were no large-scale comparative genomic analysis studies only targeting *B. glumae*, and accompanying physiological experiments. We conducted this study to understand the genomic diversity of *B. glumae* by analyzing and comparing the genomes of *B. glumae* isolates, and to find out how these genetic characteristics affect the physiology of *B. glumae*. We comparatively analyzed the genomes of 36 Korean isolates and 8 previously known isolates of *B. glumae*, and investigated the physiological traits of the Korean isolates. No significant differences in QS-dependent physiological traits, such as virulence, biosynthesis of toxoflavin, oxalate, and QS signals, were found among the 36 isolates. However, depending on

the genome structure, spontaneous *qsmR* mutants appeared at various frequencies in closed batch culture of isolates after the stationary phase, and daily supplementation of the batch culture with carbon sources reduced the frequency of *qsmR* mutant appearance. These results provide insight into how *B. glumae* evolves in harsh environments, as well as how this adaptive evolution leads to QS-defective phenotypes.

MATERIALS AND METHODS

I. Bacterial strains and growth conditions

The bacterial isolates used in this study are listed in Table 1. *B. glumae* isolates were grown in LB broth [0.1% tryptone, 0.5% yeast extract, and 0.5% NaCl (w/v); USB, Cleveland, OH, USA] or in LB broth buffered with 100 mM HEPES (pH 7.0) at 37 ℃. When necessary, the LB broth was daily supplemented with 2% glucose and 5% casamino acid for growth experiments.

Table 1. *B. glumae* isolates used in this study.

Isolate	Genome size (bp)		No. of plasmids	GC%	Geographical origin[a]	Accession number
	Chr. 1	Chr. 2				
BGR1	3,911,671	2,826,231	4	68		SAMN02603166
BGR33S	3,791,140	2,812,129	2	68	Haenam-gun, Jeollanam-do	SAMN29352428
BGR39S	3,726,678	2,828,244	4	68	Chungju-si, Chungcheongbuk-do	SAMN29352429
BGR49S	3,912,005	2,828,244	4	68		SAMN29352430
BGR57S	3,912,005	2,828,244	4	68	Changnyeong-gun, Gyeongsangnam-do	SAMN29352431
BGR59S	3,912,005	2,828,244	4	68	Goryeong-gun, Gyeongsangbuk-do	SAMN29352432
BGR68S	3,912,005	2,828,244	4	68	Bonghwa-gun, Gyeongsangbuk-do	SAMN29352433
BGR73S	3,912,005	2,828,244	4	68	Hapcheon-gun, Gyeongsangnam-do	SAMN29352434
BGR82S	3,912,005	2,828,244	4	68	Muju-gun, Jeollabuk-do	SAMN29352435
BGR85S	3,738,765	2,820,186	3	68	Naju-si, Jeollanam-do	SAMN29352436
BGR86S	3,625,957	2,852,417	5	68	Suwon-si, Gyeonggi-do	SAMN29352437
R5	3,673,124	2,846,341	3	68	Sacheon-si, Gyeongsangnam-do	SAMN29352438
SL-947S	3,738,765	2,820,186	3	68		SAMN29352439
ATCC33617*	3,659,771	2,820,414	2	68	Ehime, Japan	SAMN03012983

Continued on following pages

Table 1 – *Continued*

FDAARGOS_949*	3,659,799	2,820,518	2	68		SAMN13450479
FDAARGOS_921*	3,659,785	2,820,468	2	68		SAMN13450451
TW34RS	3,912,005	2,828,244	4	68	Gimje-si, Jeollabuk-do (Tomato)	SAMN29352440
PERW1RS	3,912,004	2,828,243	4	68	Buyeo-gun, Chungcheongnam-do (Perilla)	SAMN29352441
PW30RS	3,912,005	2,872,561	4	68	Hadong-gun, Gyeongsangnam-do (Pepper)	SAMN29352442
EW10RS	3,912,005	2,828,244	4	68	Seocheon-gun, Chungcheongnam-do (Eggplant)	SAMN29352443
SW2RS	3,912,006	2,828,245	4	68	Jecheon-si, Chungcheongbuk-do (Sunflower)	SAMN29352444
POW17RS	3,912,004	2,828,243	4	68	Yeongam-gun, Jeollanam-do (Potato)	SAMN29352445
SEW1RS	3,912,006	2,828,245	4	68	Buan-gun, Jeollabuk-do (Sesame)	SAMN29352446
BGR15S	3,742,794	2,880,619	4	68	Cheongju-si, Chungcheongbuk-do	SAMN10390411
BGR19S	3,690,419	2,852,417	3	68	Hadong-gun, Gyeongsangnam-do	SAMN29352447
BGR22S	3,827,400	2,836,302	4	68	Buan-gun, Jeollabuk-do	SAMN29352448
BGR28S	3,779,053	2,796,013	4	68	Gyeongsan-si, Gyeongsangbuk-do	SAMN29352449
BGR35S	3,702,773	2,834,421	4	68	Miryang-si, Gyeongsangnam-do	SAMN29352450

Continued on following pages

Table 1 – *Continued*

BGR76S	3,593,726	2,880,619	4	68	Namwon-si, Jeollabuk-do	SAMN29352451
YH8	3,764,216	2,908,152	3	68	Goseong-gun, Gangwon-do (diseased broken rice)	SAMN29352452
GX*	3,712,850	2,750,046	3	68	GuangXi, China	SAMN13005961
BGR21S	3,815,313	2,787,956	3	68	Changwon-si, Gyeongsangnam-do	SAMN10390410
BGR79S	3,734,736	2,783,927	4	68	Jangsu-gun, Jeollabuk-do	SAMN29352453
HN2*	3,532,897	2,745,532	1	68	Hunan, China	SAMN13005960
257sh-1*	3,537,953	2,763,738	2	68	Louisiana, USA	SAMN10913710
BGR48S	3,625,957	2,735,580	4	68	Suwon-si, Gyeonggi-do	SAMN29352454
R2	3,651,865	2,728,074	3	68	Haman-gun, Gyeonsangnam-do	SAMN29352455
R93	3,644,544	2,808,990	2	68	Taean-gun, Chungcheongnam-do	SAMN29352456
AU6208*	3,629,551	2,779,201	1	68		SAMN13567886
HN1*	3,611,155	2,869,204	3	68		SAMN14694445
SL-2395S	3,775,023	2,840,330	2	68		SAMN29352457
BGR13S	4,105,390	2,248,089	3	68	Gangjin-gun, Jeollanam-do	SAMN10390412

Continued on following pages

Table 1 – *Continued*

BGR80S	6,450,182	4	68	Suwon-si, Gyeonggi-do	SAMN10390413
BGR81S	6,490,471	4	68	Icheon-si, Gyeonggi-do	SAMN29352458

[a]Hosts from which the strain was isolated are in parentheses; all unmarked cases were isolated from diseased rice panicles. *Isolates used only for comparative genome analysis.

II. Genome sequencing and assembly

Thirty-three *B. glumae* isolates originating from South Korea were sequenced using PacBio RS-II single molecule real-time (SMRT) technology. The SMRTbell library was subjected to size selection for quality control using the BluePippin system. PacBio reads were assembled, once with HGAP v. 3 (Chin et al., 2013). HGAP3 was run on SMRT analysis v.2.3.0 and protocol RS HGAP assembly.3 with data of all four SMRT cells (default parameters, except estimated genome size: 7.35 Mb). Following draft assembly, contigs were analyzed for terminal overlaps with Circlator. Overlapping regions were trimmed and the resulting circular chromosomes and plasmids were reoriented and cut such that the origin of replication was at the start: chromosome 1 was started at the 100 bp upstream of *dnaA* gene, and chromosome 2 and plasmids were at the 100 bp upstream of *parA* gene. Circularized and reoriented was polished with Quiver (Chin et al., 2013) with SMRT cells again. The genomic DNA of strains R2, R5, and R93 was extracted using a previously published method (Sambrook et al., 1989) and sequenced using PacBio RSII and the Illumina platform (Illumina, San Diego, CA, USA). The datasets were assembled using FALCON-integrate (v2.1.4, https://pb-falcon.readthedocs.io/en/latest/). Complete genome sequences of eight strains (ATCC33617, FDAARGOS_949, FDAARGOS_921, GX, HN1, NH2, 257sh-1, AU6208) were downloaded from NCBI (20 April 2021) for comparative analysis.

III. Phylogenetic analysis

Phylogenetic analysis was carried out based on the chromosomal sequence homology. Plasmid sequences were not used for this analysis. Average nucleotide identity based on BLAST (ANIb) values was calculated using the JSpecies Standalone JAVA program (V1.2.1). A file created in Newick tree format by the hclust (hierarchical clustering) method in R software (R Development Core Team, Vienna, Austria), drawn using MegaX, was used to generate a phylogenetic tree.

IV. Comparative genomic analyses

Chromosome sequences were used for synteny and single nucleotide polymorphism (SNP) analyses. Synteny and SNP data were analyzed using the dnadiff program of the MUMmer package v4.0. A synteny map was drawn using Python script based on the MUMmer analysis. All 44 *B. glumae* genome sequences were employed for a pan- and core-genome analyses, using the pan-genomes analysis pipeline (PGAP) v1.1 (Zhao et al., 2012) and the Gene Family method with 75% identity and 50% coverage options.

V. Kanamycin resistance

After dilution of *B. glumae* isolates cultured in LB broth, spotting of the diluted culture solution on agar medium containing kanamycin was performed to confirm whether the bacteria could grow in the medium with antibiotics. In the antibiotics resistance assay, kanamycin was used at a concentration of 50 mg/mL. The kanamycin resistance gene was confirmed by an NCBI DB search for the nucleotide sequence of the long insertion region from the BLAST result for isolates with

kanamycin resistance.

VI. Virulence assay

The bacterial cells [1×10^8 colony forming units (CFU)/mL] were inoculated into Milyang-23 rice plants to assess virulence. The plants were kept in a growth chamber for 7 days at 30°C with a 16-h/8-h light/dark regime for virulence testing. The disease index was calculated using ImageJ 1.53a software (NIH, Bethesda, MD, USA) by quantifying pixels in the diseased area. The relative disease index was calculated by comparison with wild type values (disease index = disease pixels/disease pixels from the wild type). The virulence assay was repeated three times with three independent replicates.

VII. Toxoflavin and QS signal detection

Toxoflavin was extracted with chloroform and the supernatant of *B. glumae* isolates in a ratio of 1 to 1. The solvent was evaporated and the residues was reconstituted in 20 ul of methanol. Samples were applied to TLC Silica gel 60 F254 plates (Merck), and chromatograms were developed with chloroform/methanol (95:5, v/v). After development, the plate was imaged via ChemiDoc MP imaging system (Bio-Rad) and ImageLab software (version 4.0, Bio-Rad). QS signal was extracted with ethyl acetate and the supernatant of *B. glumae* isolates in a ratio of 1 to 1. The solvent was evaporated and the residue was reconstituted in 10 ul of DMSO (Dimethyl Sulfoxide). Samples were applied to TLC Silica gel 60 RP-18 F254S plates (Merck), and chromatograms were developed with methanol/water (70:30,

v/v). After development, the dried plates were over-laid with soft LB agar containing *Chromobacterium* indicator strain incubated overnight. The overlaid plates were incubated at 28℃ overnight. A toxoflavin and QS signal detection assay methods have been introduced previously (Kim et al., 2004).

VIII. Bacterial population and extracellular pH assay

Bacterial population and extracellular pH were monitored as described previously (Goo et al., 2021). Overnight cultures were washed with fresh LB broth, and an optical density (OD) of 0.05 was adjusted at 600 nm using a BioSpectrometer (Eppendorf). To monitor colony-forming units (CFUs), aliquots were serially diluted and 10 μl of three repeats was spotted on LB agar medium at the appointed time point. LB agar plates were incubated overnight at 37˚C, and CFUs were counted under a dissecting microscope. For extracellular pH assay, the culture supernatant was sampled at the appointed time point and the pH was measured via a pH meter (Lab 860, SCOTT Instruments).

IX. Measurements of ammonia and oxalate levels

Ammonia was detected using a gas-sensing ammonia ion-selective electrode (Thermo Scientific) with addition of the alkaline reagent. Oxalate was measured using an oxalate assay kit (Libios), and the absorbance at 590 nm was measured. The methods of measuring levels of ammonia and oxalate have been introduced previously (Goo et al., 2012).

X. Identification of the mutations in spontaneous null mutants

Chromosomal DNA was isolated from 21 spontaneous mutants cultured in LB broth as described previously (Sambrook et al., 1989). Based on our previous studies and the phenotypes of spontaneous null mutants, the *tofIR*, *qsmR*, and *obcAB* genes were selected as gene mutation candidates. We amplified the *tofIR*, *qsmR*, and *obcAB* gene regions of 21 mutants using the tofI-F, tofR-R, qsmR-F, qsmR-R, obcA-F, and obcb-R primers (Table 2). The PCR products were compared with the sequence of the original strain after confirming the sequence through direct sequencing at Macrogen (Seoul, South Korea). No mutations were identified in the *tofIR* or *obcAB* gene regions. Mutations in the *qsmR* gene representing four different mutation types, i.e., insertion, small deletion, medium deletion, and large deletion, were detected. We confirmed the position of 29 insertion mutants, 2 small deletion mutants, 3 medium deletion mutants, and 1 large deletion mutant by direct sequencing.

Table 2. List of primers used in this study

Primers	Sequence (5' to 3')
tofI-F	TCAGGCCGCTTCGGGTTGCGACGCGCAA
tofR-B-R	TTTGGATCCGAATGACGCGCCCATGAG
qsmR-F	GGAAATGAGGGAGACCAGTCTGTCT
qsmR-R	CTTTCTTTCGACCGTTTACGGCGG
B-obcA-F	AGCTAGCGGATCCGGACGGATGGGGTCCGATTTTCGG
obcB-E-R	CATGCATGAATTCTCACCGCGTCACGCGTACCAGCT

F- forward primer; R- reverse primer

RESULTS

I. Identification and genome sequencing of *B. glumae* isolates

B. glumae isolates were collected from all provinces of South Korea, including Gyeonggi-do, Gyeongsang-do, Jeolla-do, Chungcheong-do, and Gangwon-do (Table 1). Among 36 *B. glumae* isolates, 28 samples were isolated from diseased rice panicles, and YH8 was isolated from diseased broken rice. The other seven samples—TW34RS, PERW1RS, PW30RS, EW10RS, SW2RS, POW17RS, and SEW1RS—were from Solanaceous crops such as tomato, perilla, pepper, eggplant, sunflower, potato, and sesame (Table 1). Among the 36 Korean *B. glumae* isolates, the complete genome sequence of strain BGR1 had been determined previously (Lim et al., 2009). The remaining 35 isolates shared more than 99% identity with *B. glumae* based on 16S rRNA analysis, and the complete genome sequences of these isolates were determined. The genomes of the 35 isolates ranged in size from 6.5 to 7.3 Mbp, with a G + C content of 68% (Table 1). Unlike the other isolates that have two chromosomes, BGR80S and BGR81S have one large chromosome (Table 1). The number of plasmids in the *B. glumae* isolates varied from one to five (Table 1).

II. Comparative genome analysis of *B. glumae* isolates

To determine whether the *B. glumae* strains from different hosts and regions have genomic diversity, the genomes of 44 isolates were comparatively analyzed. Based on a

phylogenetic analysis comparing chromosome sequence homology, the 44 isolates were classified into six clusters and two divisions; division I contained clusters I–IV, while clusters V and VI were in division II (Figure 1). Strain BGR1 and the isolates from Solanaceous crops were in cluster I; BGR35S, BGR49S, and R5 were in cluster II; BGR80S and BGR81S were in cluster III; YH8 isolated from diseased broken rice and BGR15S were in cluster IV; HN1, 257sh-1, GX, and the clinical isolate AU6208 were in cluster V; BGR13S and BGR21S were in cluster VI (Figure 1). Pan-genome analysis via PGAP identified 13,298 orthologs in all isolates (Figure 2). Among them, 4,143 orthologs were highly conserved, constituting the core genome (Figure 2). Another 4,096 orthologs were identified as dispensable, while the individual genomes contained 52 to 329 strain-specific genes (Figure 2).

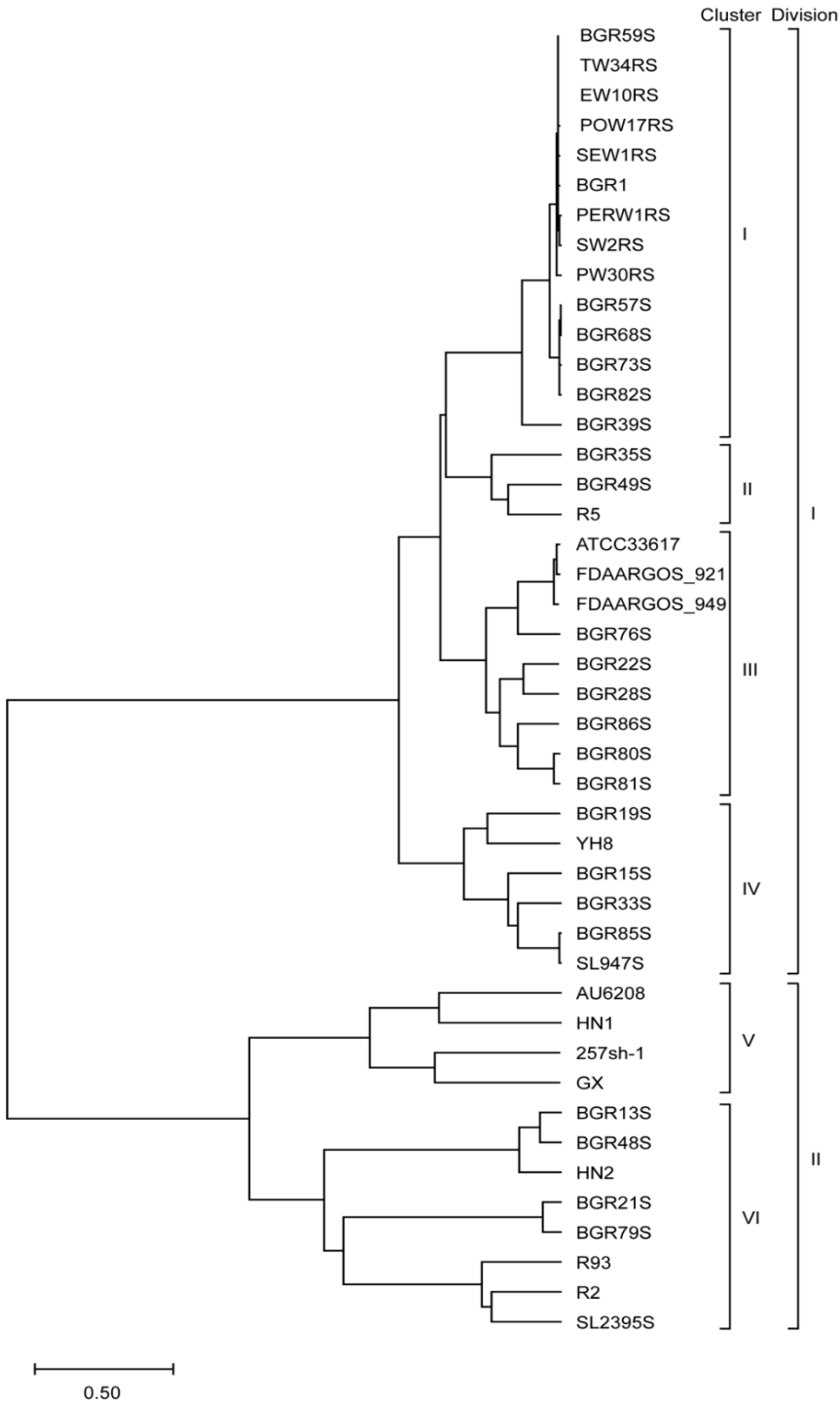
Cluster
Division
BGR59S
TW34RS
EW10RS
POW17RS
SEW1RS
BGR1
PERW1RS
SW2RS
PW30RS
BGR57S
BGR68S
BGR73S
BGR82S
BGR39S
BGR35S
BGR49S
R5
ATCC33617
FDAARGOS_921
FDAARGOS_949
BGR76S
BGR22S
BGR28S
BGR86S
BGR80S
BGR81S
BGR19S
YH8
BGR15S
BGR33S
BGR85S
SL947S
AU6208
HN1
257sh-1
GX
BGR13S
BGR48S
HN2
BGR21S
BGR79S
R93
R2
SL2395S
I
II
III
IV
V
VI
I
II
0.50

Figure 1. Phylogenetic analysis of *B. glumae* isolates based on the homology of two chromosome sequences. According to their sequence homology, 44 *B. glumae* genomes were classified into two divisions and six clusters.

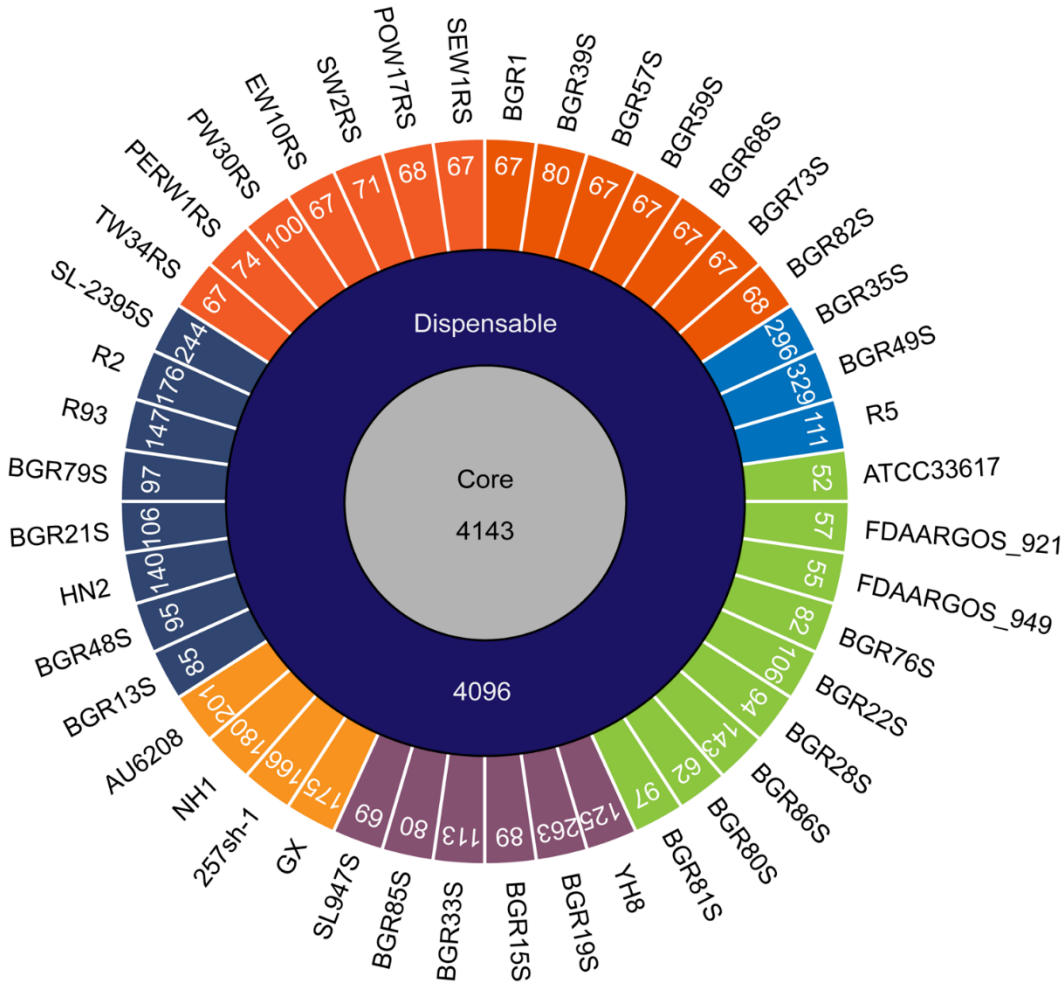

Figure 2. Pan-genome analysis of *B. glumae* isolates. The numbers inside the circular diagram indicate the numbers of core, dispensable, and unique genes. The unique genes of each isolate are colored according to their phylogenetic classification; cluster I, orange; cluster II, blue; cluster III, green; cluster IV, purple; cluster V, light-orange; cluster VI, navy.

III. Genomic structural variation across *B. glumae* isolates

Synteny analysis was performed on the assembled sequences to improve the gene annotation of the 35 newly sequenced isolates, and to study the genomic evolution in all 44 isolates. Using structural homologies of the genome, the 44 isolates were divided into seven groups, represented by isolates BGR1, BGR15S, BGR21S, HN2, 257sh-1, BGR13S, and BGR80S. The BGR1 group consisted of isolates with a similar genome structure to the prototype BGR1 (Figure 3A). The isolates of the BGR15S group had one inversion on chromosome 1g (except isolate GX, which had two inversions), as well as several deletions in the genome (Figure 3B). In the BGR21S group, BGR21S and BGR79S also had one inversion on chromosome 1g, but there was a sequence discrepancy with BGR1, with sequence homologies of 99.18% (BGR21S) and 99.21% (BGR79S) (Figure 3C). The HN2 group isolates had an inversion on chromosome 2g, as well as several deletions in the genome (Figure 3D). The 257sh-1 group isolates each had inversions on chromosomes 1g and 2g, but the inversion positions were all different; strain R93 had one inversion on chromosome 1g and three on chromosome 2g (Figure 3E). Compared to BGR1, the BGR13S group isolates had rearrangements at 24 positions between chromosomes 1g and 2g (Figure 3F). The BGR80S group isolates possessed two chromosomes that were merged into one (Figure 3G).

A. BGR1 group

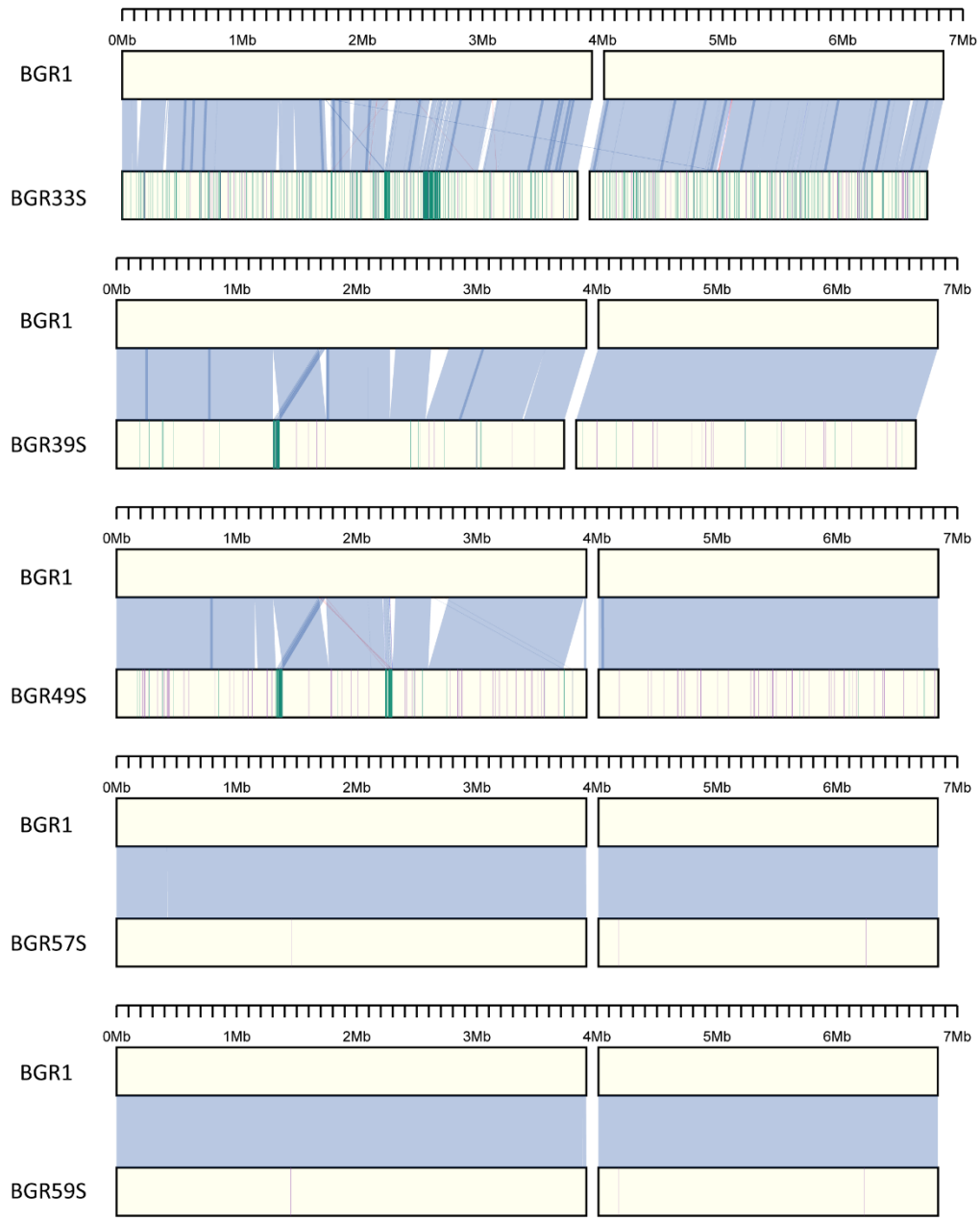
0Mb
1Mb
2Mb
3Mb
4Mb
5Mb
6Mb
7Mb
BGR1
BGR33S
BGR1
BGR39S
BGR1
BGR49S
BGR1
BGR57S
BGR1
BGR59S

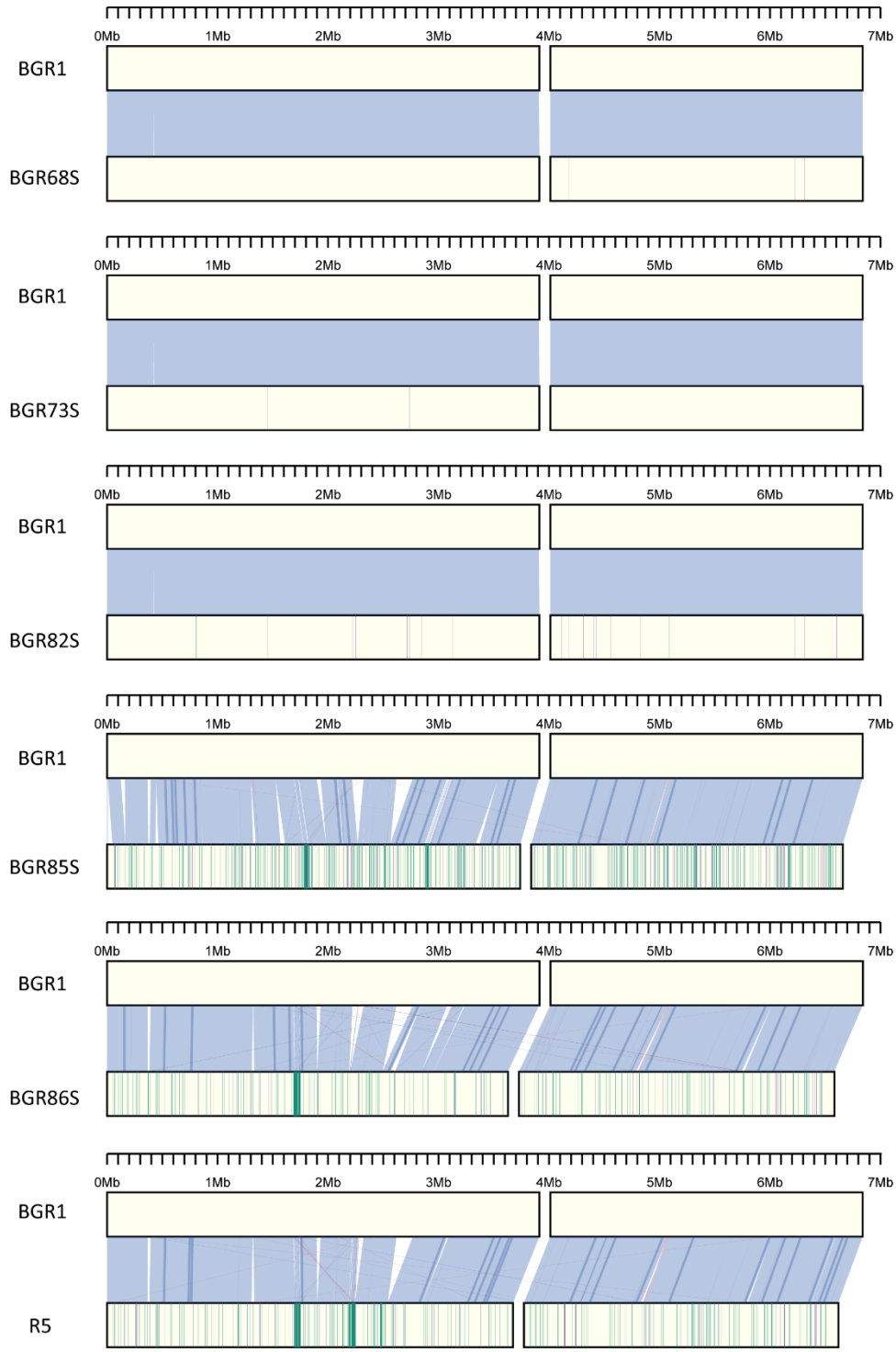
0Mb
1Mb
2Mb
3Mb
4Mb
5Mb
6Mb
7Mb
BGR1
BGR68S
BGR1
BGR73S
BGR1
BGR82S
BGR1
BGR85S
BGR1
BGR86S
BGR1
R5

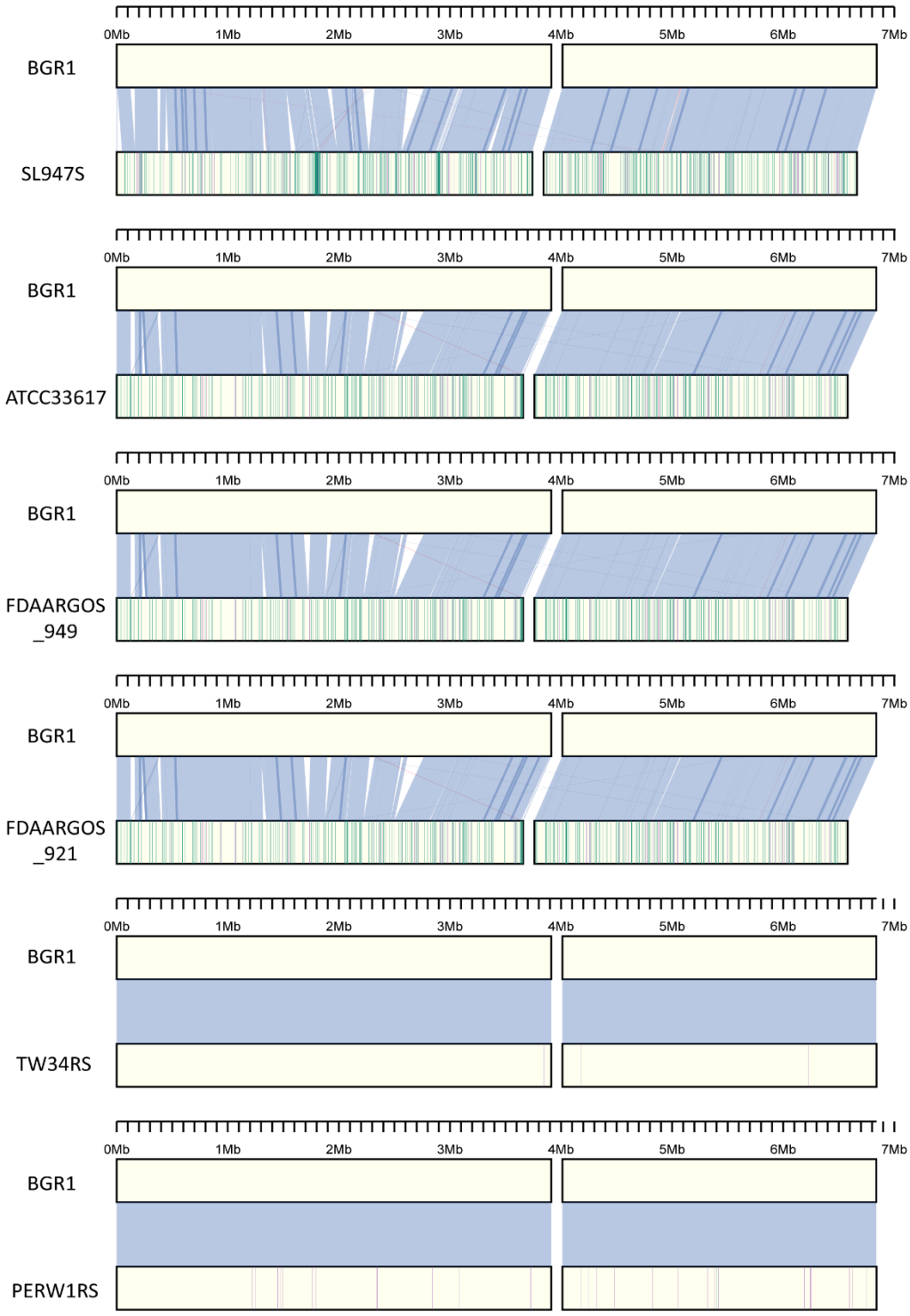
0Mb
1Mb
2Mb
3Mb
4Mb
5Mb
6Mb
7Mb
BGR1
SL947S
BGR1
ATCC33617
BGR1
FDAARGOS_949
BGR1
FDAARGOS_921
BGR1
TW34RS
BGR1
PERW1RS

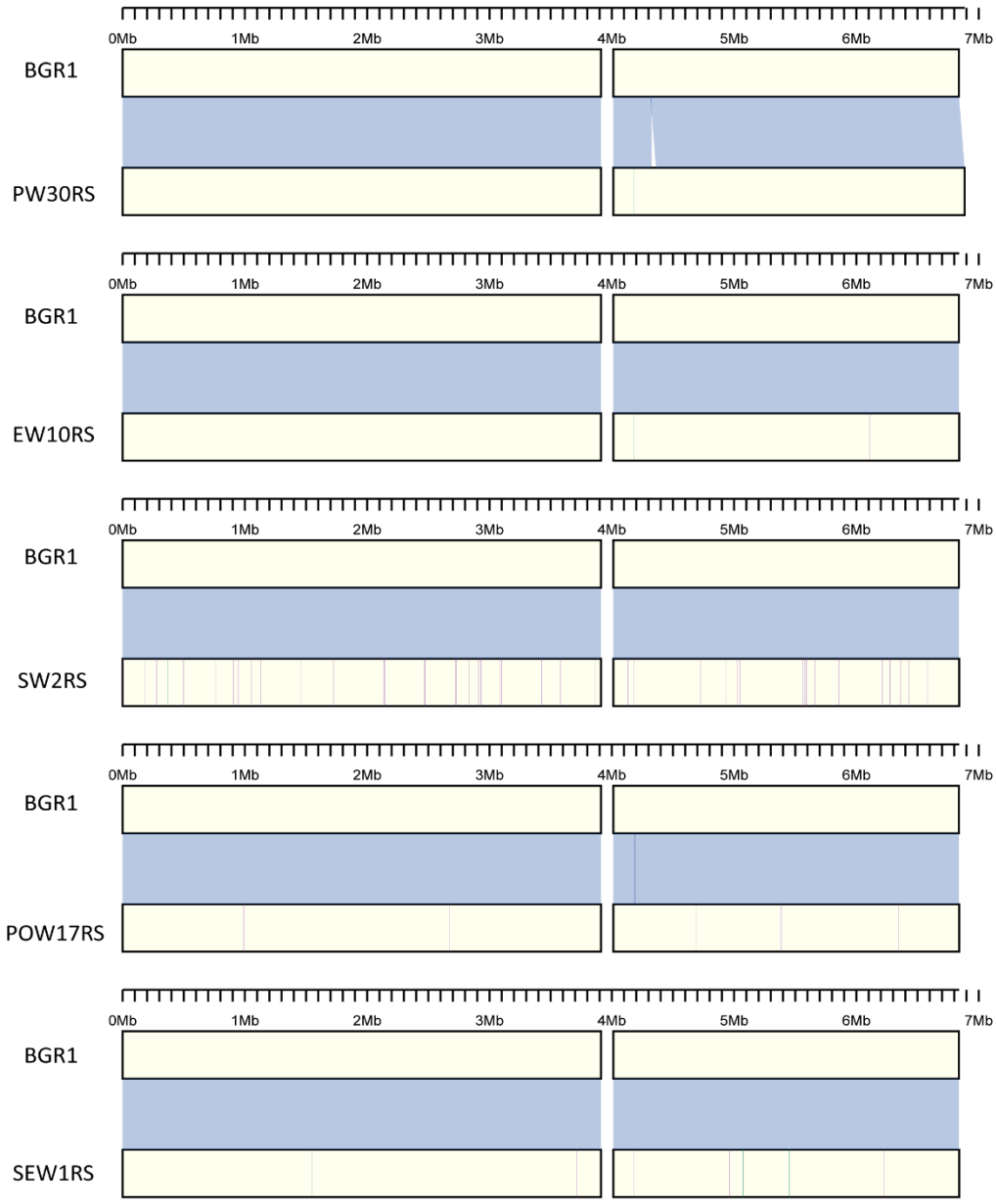
0Mb
1Mb
2Mb
3Mb
4Mb
5Mb
6Mb
7Mb
BGR1
PW30RS
BGR1
EW10RS
BGR1
SW2RS
BGR1
POW17RS
BGR1
SEW1RS

B. BGR15S group

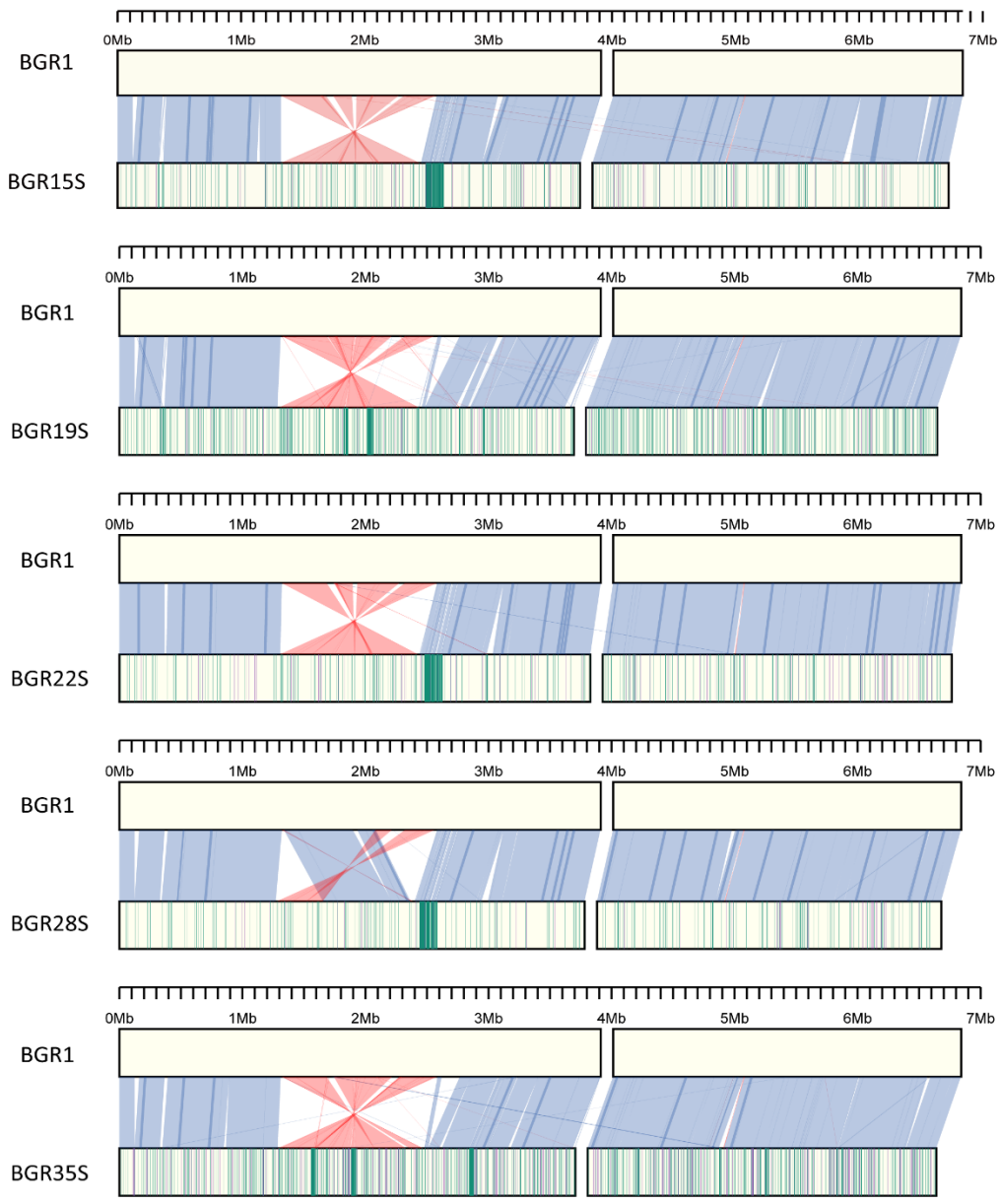

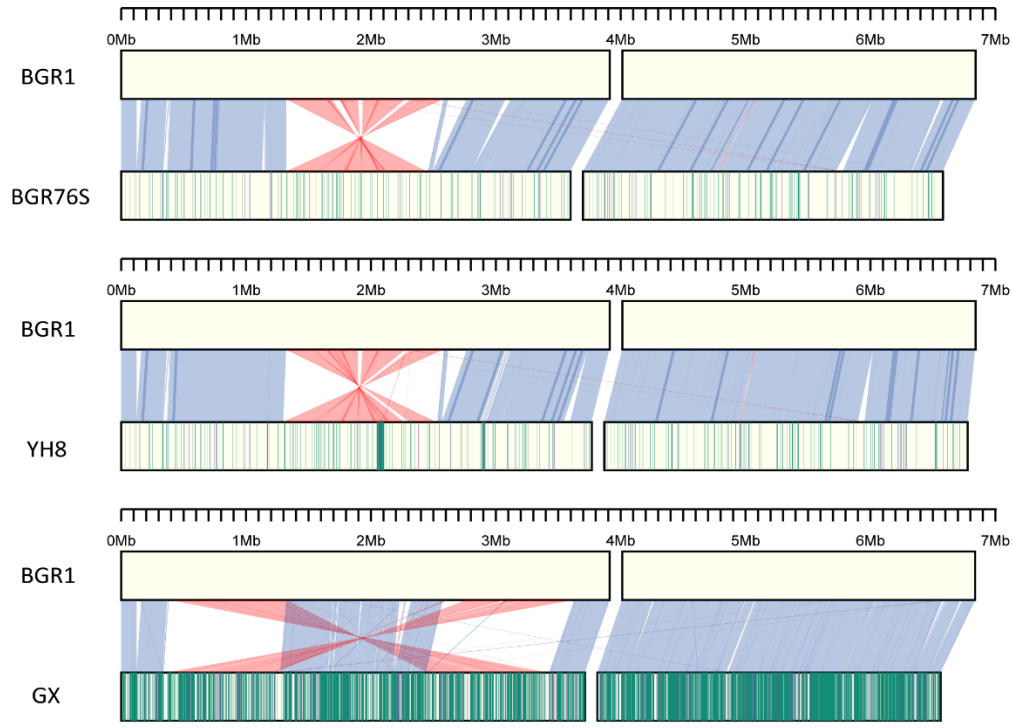

C. BGR21S group

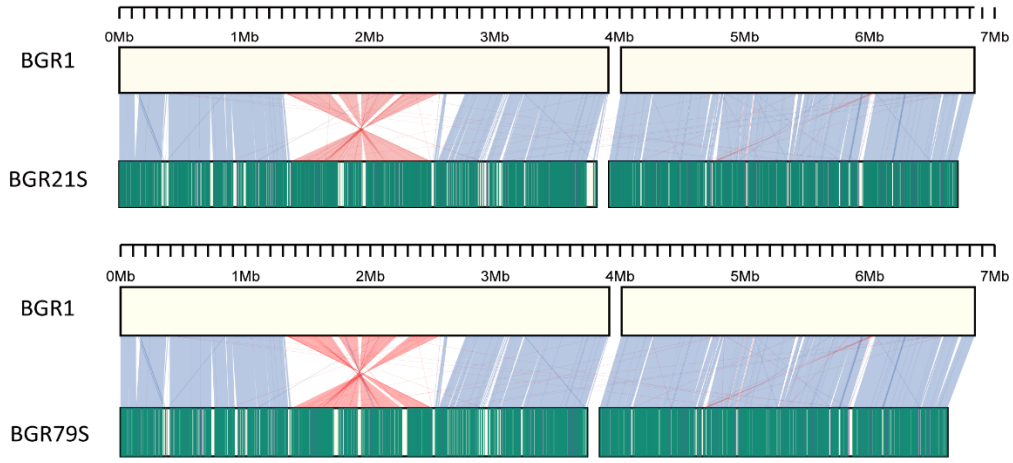

D. HN2 group

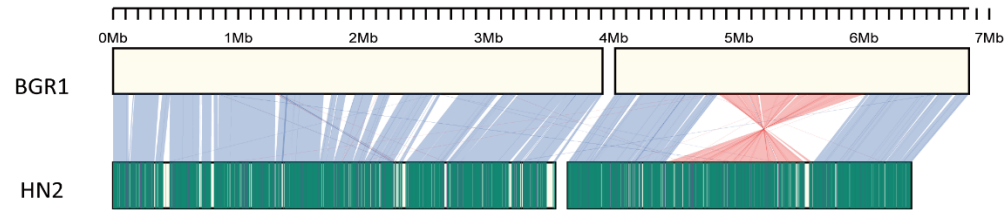

E. 257sh-1 group

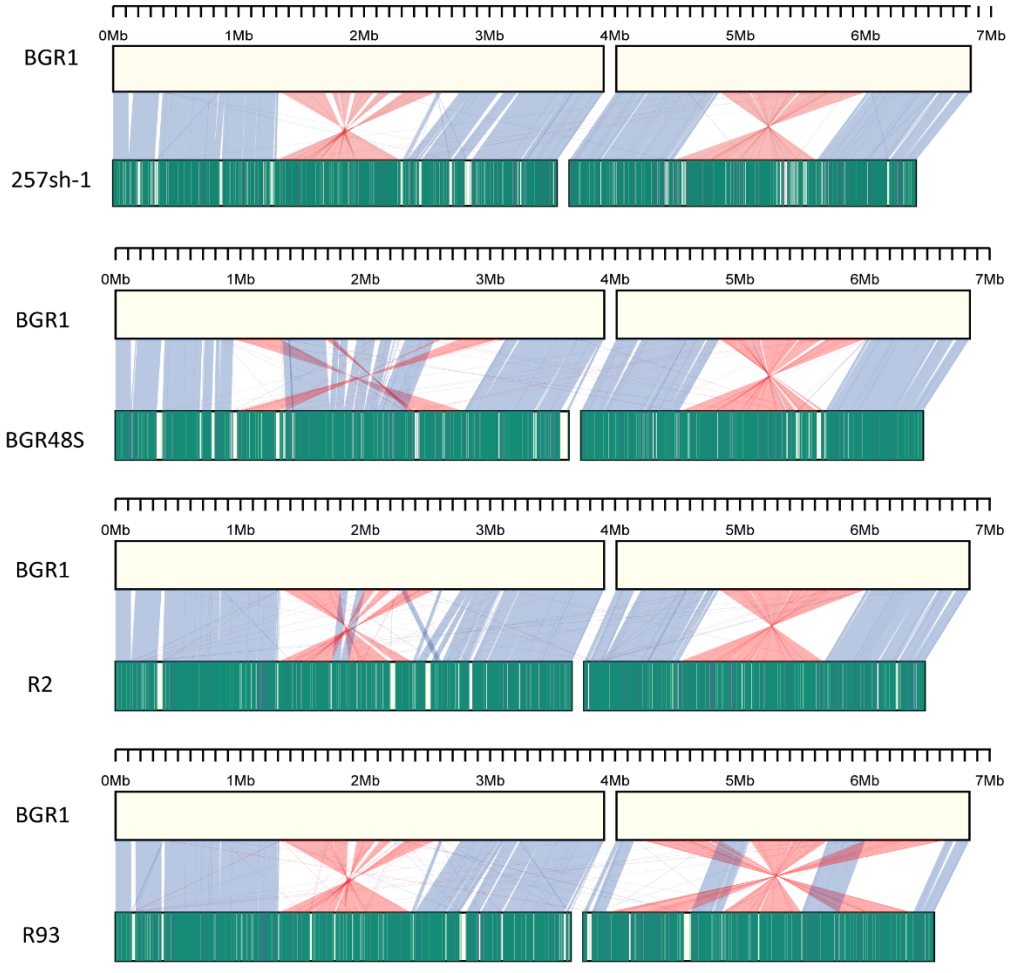

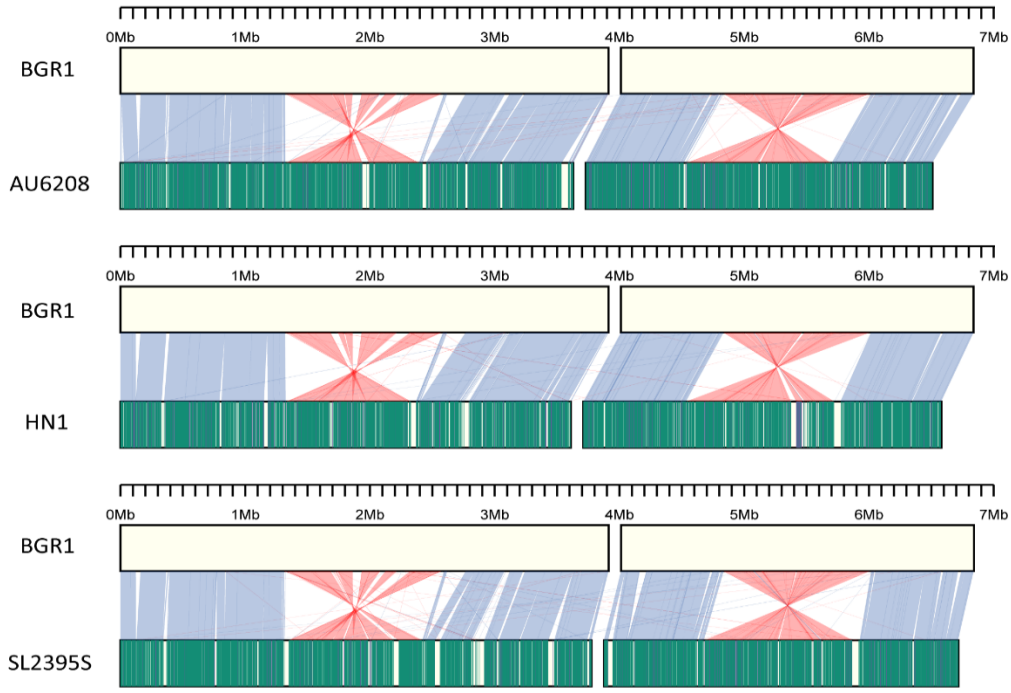

F. BGR13S group

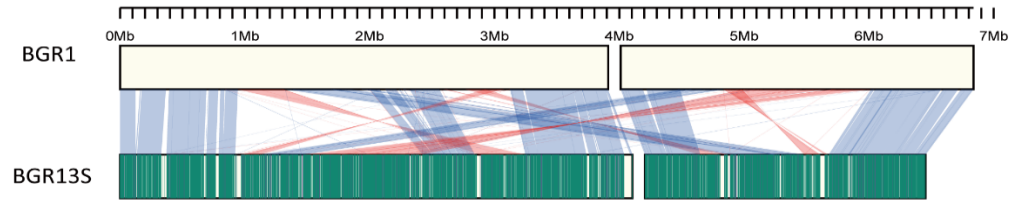

G. BGR80S group

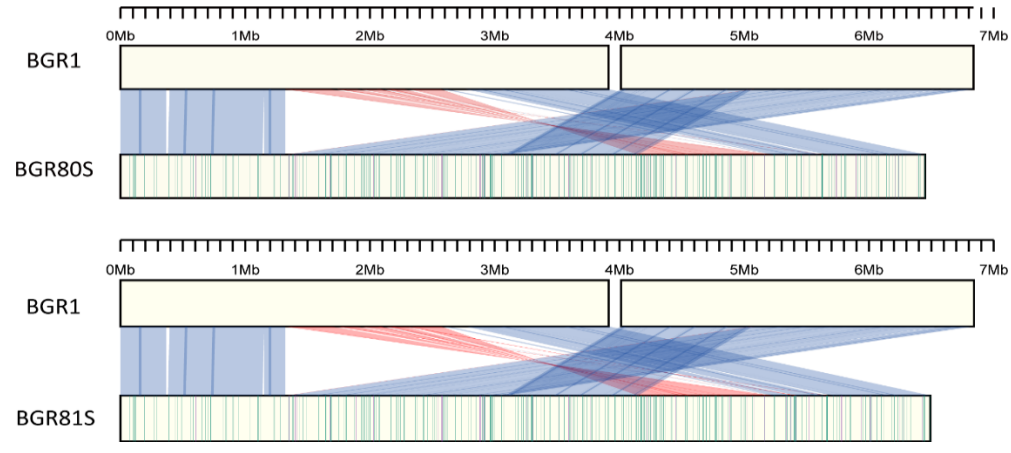

Figure 3. Synteny analysis of *B. glumae* isolates. Genome structures of each isolate are compared to BGR1. The upper part is the BGR1 genome; the lower part is the genomes of other *B. glumae* isolates. The blue lines between genomes of two different isolates show the regions corresponding to each other; the red lines show areas where inversion occurred. The vertical green lines indicate the locations of SNPs compared to BGR1; the vertical purple lines indicate INDELs. The darker color, the more SNPs or INDELs occurred.

IV. Merged two chromosomes in the BGR80S group genome

To determine how the single large chromosomes of BGR80S and BGR81S were generated, we investigated the genetic exchanges that occurred at junctions between chromosomes 1g and 2g. At one location, transposase (bglu_1g12100) and fimbrial biogenesis outer membrane usher protein (bglu_2g08800) genes were combined (Figure 4). In addition, transposases, integrases, and a 9,533-bp DNA fragment with 89% sequence identity to *Achromobacter insolitus* strain NCTC13520 were inserted between the two genes (Figure 4). In another location, the L-seryl-tRNA selenium transferase gene (bglu_2g08680) and transposase IS66 (bglu_1g23470) were merged (Figure 4). In BGR80S, a 39,497-bp sequence present in the BGR81S genome (base range: 5,377,980–5,417,476) was also deleted (Table 1). The ori1 and ori2 origins of replications were identified in BGR80S and BGR81S by homology to the chromosome 1g and 2g origins of prototype BGR1 (Figure 4).

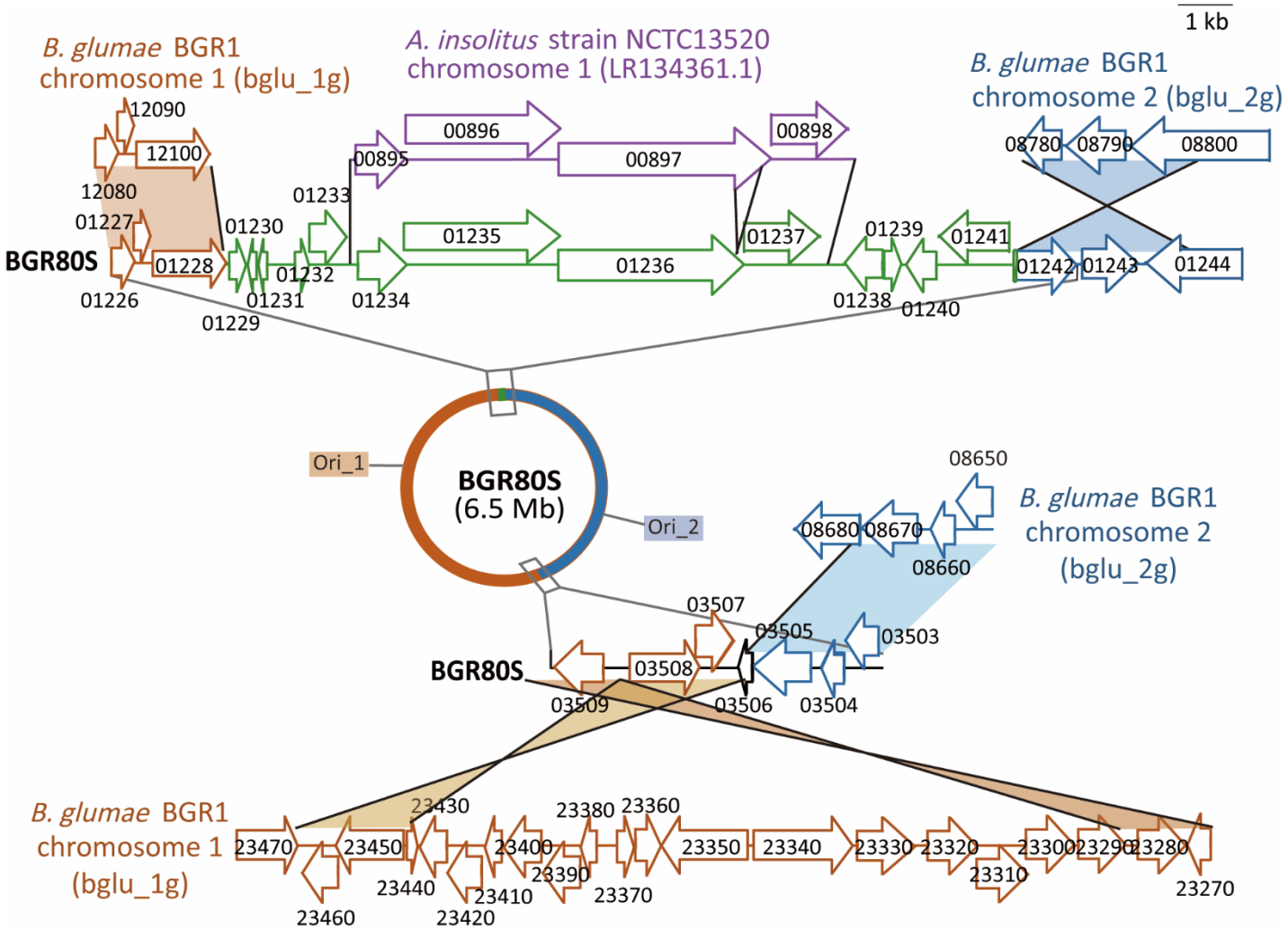
1 kb
B. glumae BGR1
chromosome 1 (bglu_1g)
A. insolitus strain NCTC13520
chromosome 1 (LR134361.1)
B. glumae BGR1
chromosome 2 (bglu_2g)
12090
12100
12080
01227
BGR80S
01228
01226
01229
01230
01231
01233
01232
00895
00896
00897
00898
01234
01235
01236
01237
01239
01241
01238
01240
08780
08790
08800
01242
01243
01244
Ori_1
BGR80S
(6.5 Mb)
Ori_2
08650
08680
08670
08660
B. glumae BGR1
chromosome 2
(bglu_2g)
03507
03505
03503
BGR80S
03508
03509
03506
03504
B. glumae BGR1
chromosome 1
(bglu_1g)
23430
23380
23360
23470
23450
23400
23350
23340
23330
23320
23300
23290
23280
23440
23390
23410
23370
23310
23460
23420
23270

Figure 4. Genetic map of the fusion junctions of two chromosomes in *B. glumae* BGR80S. The red half-circle is the region corresponding to prototype BGR1 chromosome 1 (bglu_1g); the blue half-circle is the area corresponding to BGR1 chromosome 2 (bglu_2g). On the two chromosomes of BGR1, the genes bglu_1g 12100 and bglu_2g 08800, and bglu_1g 23470 and bglu_2g 08680, merged to form the single chromosome of BGR80S. There were two replication origins in the single chromosome of BGR80S. A DNA fragment of *A. insolitus* strain NCTC13520 chromosome 1 was inserted between bglu_1g01228 and bglu_2g01242 in the BGR80S genome. The DNA fragment in purple is the original sequence from *A. insolitus* strain NCTC13520; the DNA fragment in green with some deletions was inserted into *B. glumae* BGR80S.

V. Kanamycin resistance

To examine phenotypic differences between *B. glumae* isolates, we tested for antibiotic resistance. Five isolates from cluster I—BGR57S, BGR59S, BGR68S, BGR73S, and BGR82S—exhibited resistance to kanamycin and contained the kanamycin resistance gene aminoglycoside 3'-phosphotransferase (*aphA*) in their genomes (Figure 5). The foreign DNA carrying the *aphA* gene was inserted between the bglu_1g04020 gene and bglu_1g04030 genes in BGR57S, BGR68S, BGR73S, and BGR82S (Figure 5). In BGR59S the gene was inserted into the bglu_1g34110 gene (Figure 5). BLAST analysis revealed that the inserted DNA sequence matched the plasmid pSCR001 (accession no. DQ059989) with the widest query coverage (Figure 5).

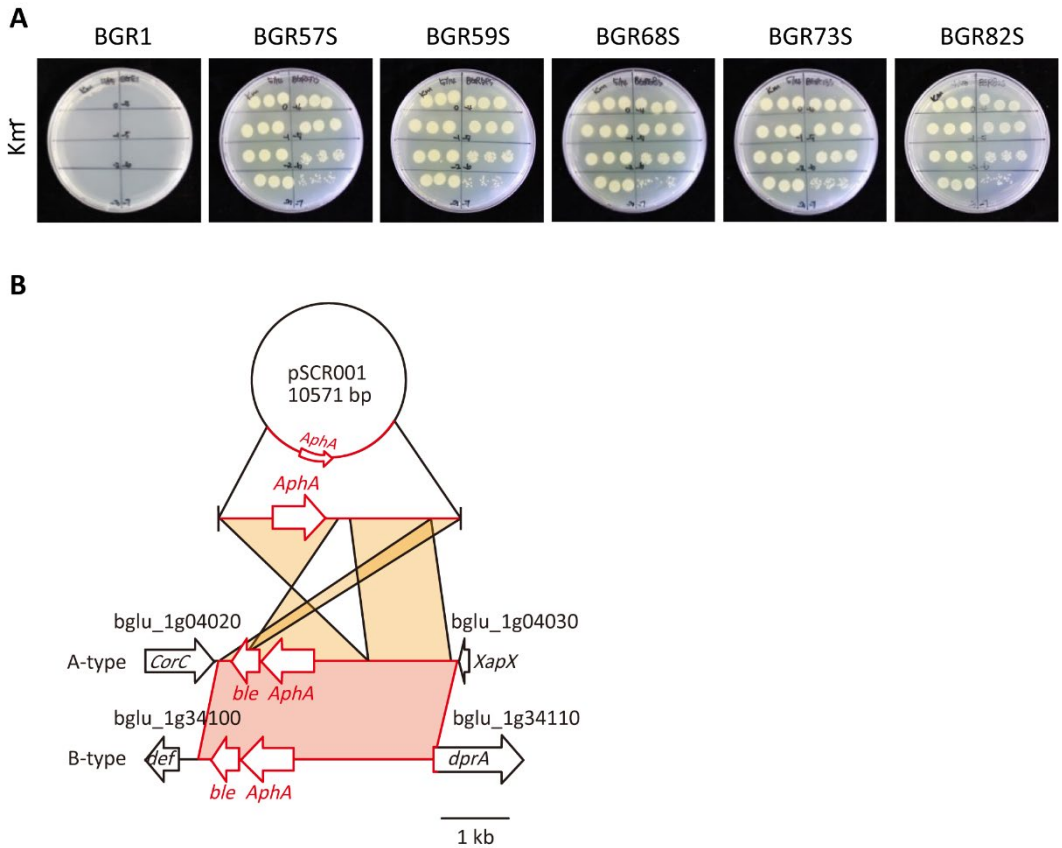

Figure 5. Kanamycin resistance and genetic map of the insertion of the kanamycin resistance gene. (A) It was observed whether the isolates could grow in LB medium containing kanamycin at a 50 mg/mL concentration. (B) A DNA fragment containing a kanamycin resistance gene (*aphA*) derived from plasmid pSCR001 was inserted in two different types of regions: A-type, between bglu_1g04020 and 1g04030 in BGR57S, BGR68S, BGR73S, BGR82S; and B-type, between bglu_1g34100 and 1g34110 in BGR59S. The DNA fragments inserted in *B. glumae* isolates showed 99% identity to pSCR001.

VI. Emergence of QS-dependent gene regulation defects

To examine the effect of genomic structural differences on the physiology of *B. glumae*, experiments were conducted to confirm pathogenicity and production of QS signals and toxoflavin. But the genomic diversity of *B. glumae* isolates did not affect their virulence, or the biosynthesis of QS signals and toxoflavin (Figures 6, 7).

So, we explored whether the genomic diversity of *B. glumae* isolates was associated with their ability to adapt to changing environments. We monitored the populations of BGR1, BGR13S, BGR15S, BGR21S, and BGR80S as representative isolates of each genome group during an 8-day incubation in LB medium, without supplementation with additional nutrients. The population density of BGR80S decreased 1 day after subculture, and was then maintained at about 3.1×10^8 CFU/mL (Figure 8A). The other three isolates showed the same growth pattern as BGR1 (Figure 8A). All five isolates exhibited the same patterns in extracellular pH (Figure 8B). However, the populations of BGR80S, BGR15S, and BGR21S were not homogeneous, containing morphologically distinct mutant colonies (Figure 8C). The mutant appeared 2 days after subculture in the BGR80S and soon accounted for ~80% of the population (Figure 8D). In BGR15S and BGR21S, the mutant was detected 6 days after subculture and reached ~40% of the population (Figure 8D). No mutant was observed at detectable frequency in BGR1 or BGR13S (Figure 8D). The mutants did not survive the stationary phase after being isolated due to the toxic alkaline extracellular pH resulting from the failure to activate oxalate biosynthesis in a QS-dependent manner, as observed previously (Figure 9). To characterize the spontaneously occurring mutant, we sequenced the *tofIR*, *qsmR*, and *obcAB* gene regions associated with

its phenotype. All 35 isolates from three experiments in which mutants accumulated had *qsmR* mutations (Figure 8E). The *qsmR* mutations arising in BGR80S, BGR15S, and BGR21S included IS element insertions, small deletions, medium deletions, and large deletion in the *qsmR* gene (Figure 8E).

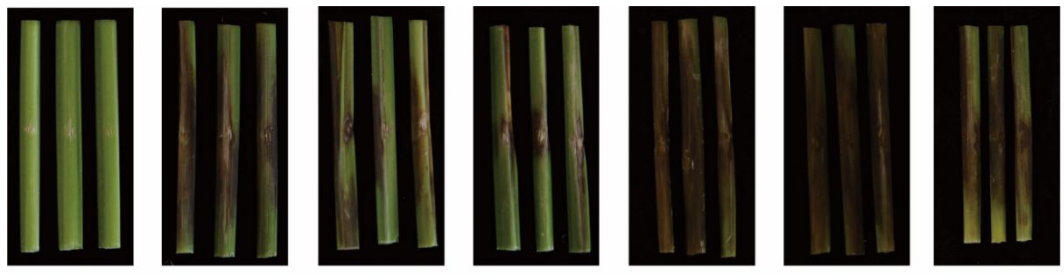

Figure 6. Virulence in rice stems of *B. glumae* isolates. Disease symptoms of the indicated *B. glumae* strains in rice stems were photographed 7 days after inoculation. The numbers below the disease symptoms are the relative disease index scored by ImageJ software by comparison with the wild type values. Data represent the mean ± standard error (SE) of triplicates.

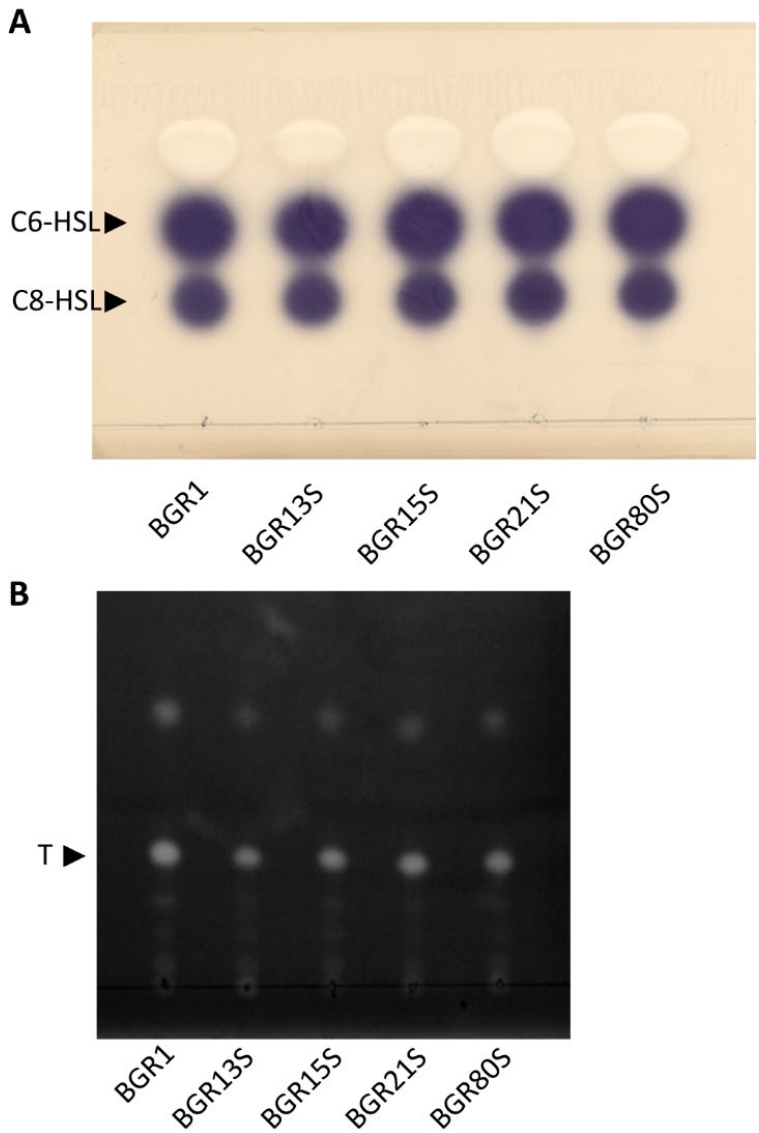

Figure 7. Autoinducers and toxoflavin production of *B. glumae* isolates. The *B. glumae* isolates produced (A) autoinducers and (B) toxoflavin to the same levels as those produced by the BGR1. C6-HSL; hexanoyl homoserine lactone, C8-HSL; octanoyl-HSL, T; toxoflavin.

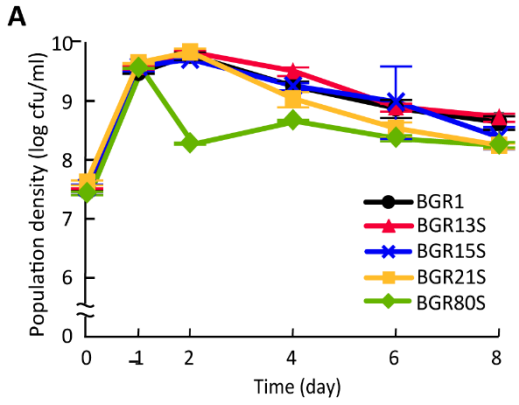
A
Population density (log cfu/ml)
Time (day)
BGR1
BGR13S
BGR15S
BGR21S
BGR80S

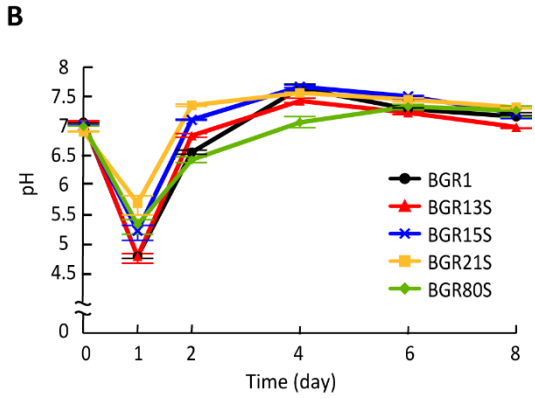
B
pH
Time (day)
BGR1
BGR13S
BGR15S
BGR21S
BGR80S

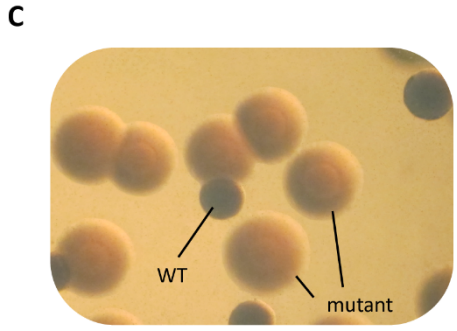
C
WT
mutant

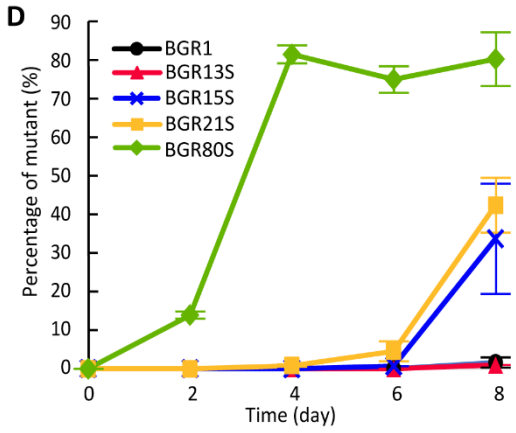
D
Percentage of mutant (%)
Time (day)
BGR1
BGR13S
BGR15S
BGR21S
BGR80S

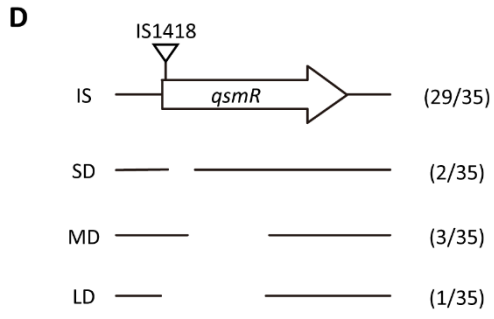
D
IS1418
IS
qsmR
(29/35)
SD
(2/35)
MD
(3/35)
LD
(1/35)

Figure 8. Cell viability, pH changes and appearance of quorum sensing-dependent gene regulation defects from *B. glumae* isolates. (A) Viable cell numbers were monitored at 1, 2, 4, 6, and 8 days after subculture and colony-forming units (CFUs) were counted. Data represent the mean ± standard error (SE) of triplicates. (B) The pH changes of *B. glumae* isolates of BGR1, BGR13S, BGR15S, BGR21S, and BGR80S. The pH was measured at 1, 2, 4, 6, and 8 days after subculture. Data represent the mean ± SE of triplicates. (C) Morphologically distinct colonies compared to the wild type colonies were observed in BGR80S culture under a dissecting microscope at 30× magnification. (D) The percentage of mutants was monitored at 2-day intervals for 8 days, and calculated by dividing the CFUs of the mutants by the total CFUs. Data represent the mean ± SE of triplicates. (E) Characterization of *qsmR* mutations in mutants emerging from BGR80S, BGR15S, and BGR21S. Among the 35 mutants, 29 had an insertion of IS1418 at the 5' end of the *qsmR* gene, and 2, 3, and 1 had 112-, 361-, and 468-bp internal deletions, respectively.

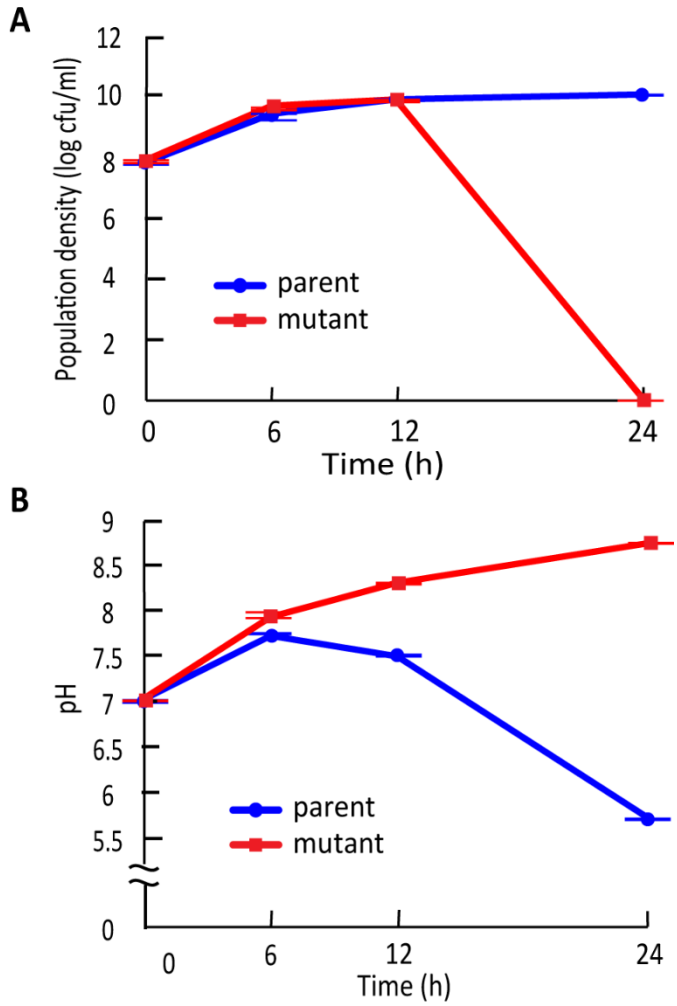

Figure 9. Cell viability and pH changes of the BGR1 and mutant. (A) Viable cell numbers and (B) pH were monitored at 6, 12, and 24 hours after subculture. Data represent the mean ± SE of triplicates.

VII. The mutant has a fitness benefit over the wild type

To determine whether the mutation in QS-dependent gene regulation confers a fitness advantage during batch culture incubation, we monitored the population density and pH in mixed culture. The mutant outcompeted the parent even when the initial mutant frequency was ~10% in fresh LB medium (Figures 10A, B). The percentage of mutants increased from 16% to 58.4%, while that of BGR80S parents decreased from 84% to 41.6% during competition in the LB medium. Whole populations collapsed in LB medium because the external pH increased to ~8.4, and viable *B. glumae* is not observed at a pH of 8.5 (Figures 10A, C). The addition of 100 mM HEPES buffer to LB medium prevented population collapse; the mutant then outgrew the parent in mixed culture, increasing from 10.4% to 75% of the whole population (Figures 10D, E).

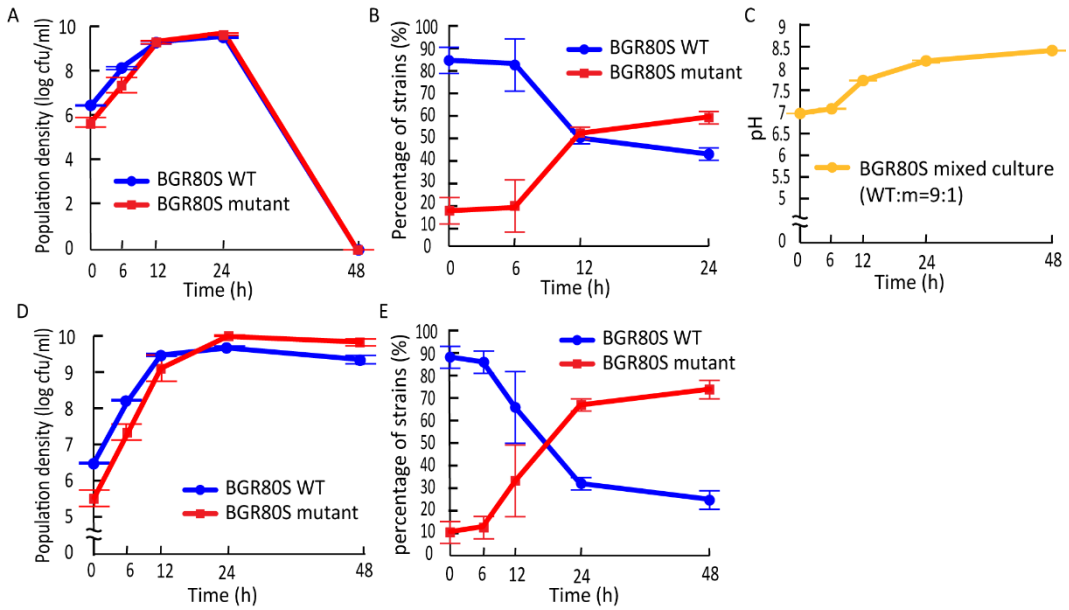

Figure 10. Competition between the parental strain BGR80S and the mutant in fresh LB or LB supplemented with 100 mM HEPES (pH 7.0). (A) Viable cell numbers of the parent and mutant in LB medium were monitored by counting CFUs at 0, 6, 12, 24, and 48 hours after subculture with an initial mutant frequency of ~10%. (B) The proportions of parent and mutant in LB medium were calculated by dividing their CFUs by the total CFUs. If no viable cells were observed 48 hours after subculture in LB medium, the percentage of strains was not counted. (C) External pH fluctuation during this experiment. (D) Viable cell numbers of the parent and mutant in LB supplemented with 100 mM HEPES (pH 7.0) were determined by counting CFUs at 0, 6, 12, 24, and 48 hours after subculture with an initial mutant frequency of ~10%. (E) The proportion of parent and mutant in LB supplemented with 100 mM HEPES (pH 7.0) were calculated by dividing their CFUs by the total CFUs. All data represent the mean ± SE of triplicates.

VIII. Daily nutrient supplementation reduces mutation incidence

In batch culture, nutrient stress may become constant from 1 day after subculture, inducing spontaneous mutations to adapt to these conditions. To test this hypothesis, on each day we added 5% casamino acids or 2% glucose to the batch culture in LB medium, to evaluate their influence on mutant incidence. Total populations of BGR1 and BGR80S grown in LB enriched with casamino acids reached a maximum and then gradually began to decrease 2 days after subculture, reaching ~7.5×10^6 CFU/mL for BGR1 and ~1.3×10^7 CFU/mL for BGR80S at seven days (Figure 11A). BGR1 and BGR80S grown in LB enriched with glucose maintained 6.0×10^9 CFU/mL and 3.8×10^9 (CFU/ml), respectively, for 7 days (Figure 11A). Spontaneous mutants were not observed from either strain grown in casamino acid-rich conditions (Figure 11B). However, in glucose-rich conditions, the mutant appeared 4 days after subculture in BGR80S and reached ~2-3% of the whole population (Figure 11B). The external pH of BGR1 and BGR80S in either casamino acids- or glucose-rich conditions was maintained at a light acidic to neutral level due to the amount of oxalate produced, even though ammonia was highly produced by both strains grown in LB supplemented with casamino acids (Figure 11C, D, E). To determine whether spontaneous mutants emerged in minimal medium, populations of BGR1 and BGR80S growing in M9 minimal medium supplemented with 0.4% glucose were monitored for 8 days. The mutant was observed in BGR80S 6 days after subculture and comprised ~40% of the total population (Figure 12).

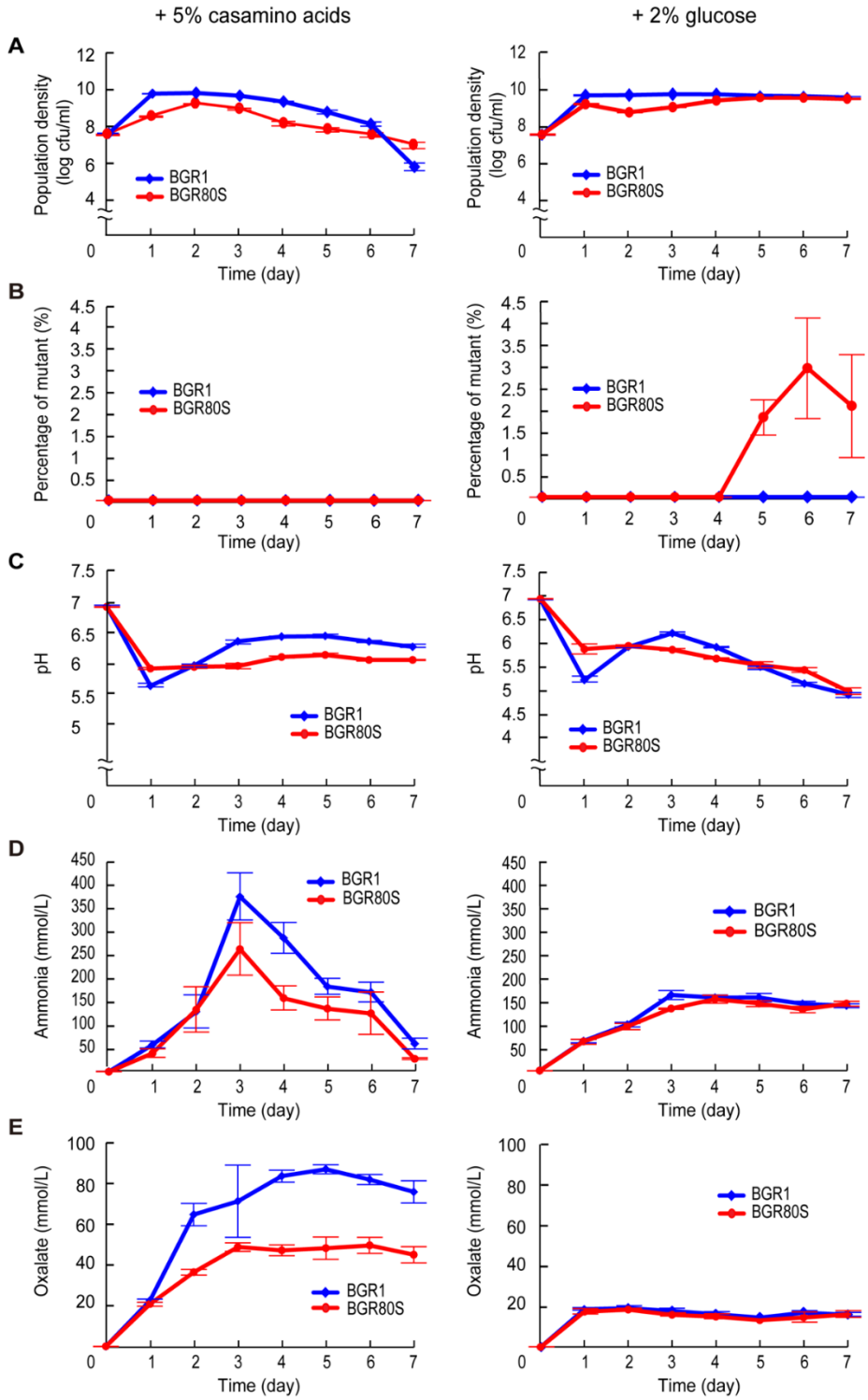
+ 5% casamino acids
+ 2% glucose
A
B
C
D
E
Population density (log cfu/ml)
Percentage of mutant (%)
pH
Ammonia (mmol/L)
Oxalate (mmol/L)
Time (day)
BGR1
BGR80S

Figure 11. Reduced mutation incidence for BGR80S in LB supplemented with 5% casamino acids or 2% glucose. (A) Viable cell numbers of BGR1 and BGR80S were monitored daily for 7 days by counting CFUs during growth in LB supplemented with 5% casamino acids or 2% glucose. (B) The percentage of mutants was calculated by dividing the CFUs of the mutant by the total CFUs during growth in LB supplemented with 5% casamino acids or 2% glucose. (C) The external pH of BGR1 and BGR80S was measured for 7 days, and (D, E) the levels of ammonia and oxalate produced by BGR1 and BGR80S were examined for the indicative days in casamino acid- or glucose-enriched LB medium. All data represent the mean ± SE of triplicates.

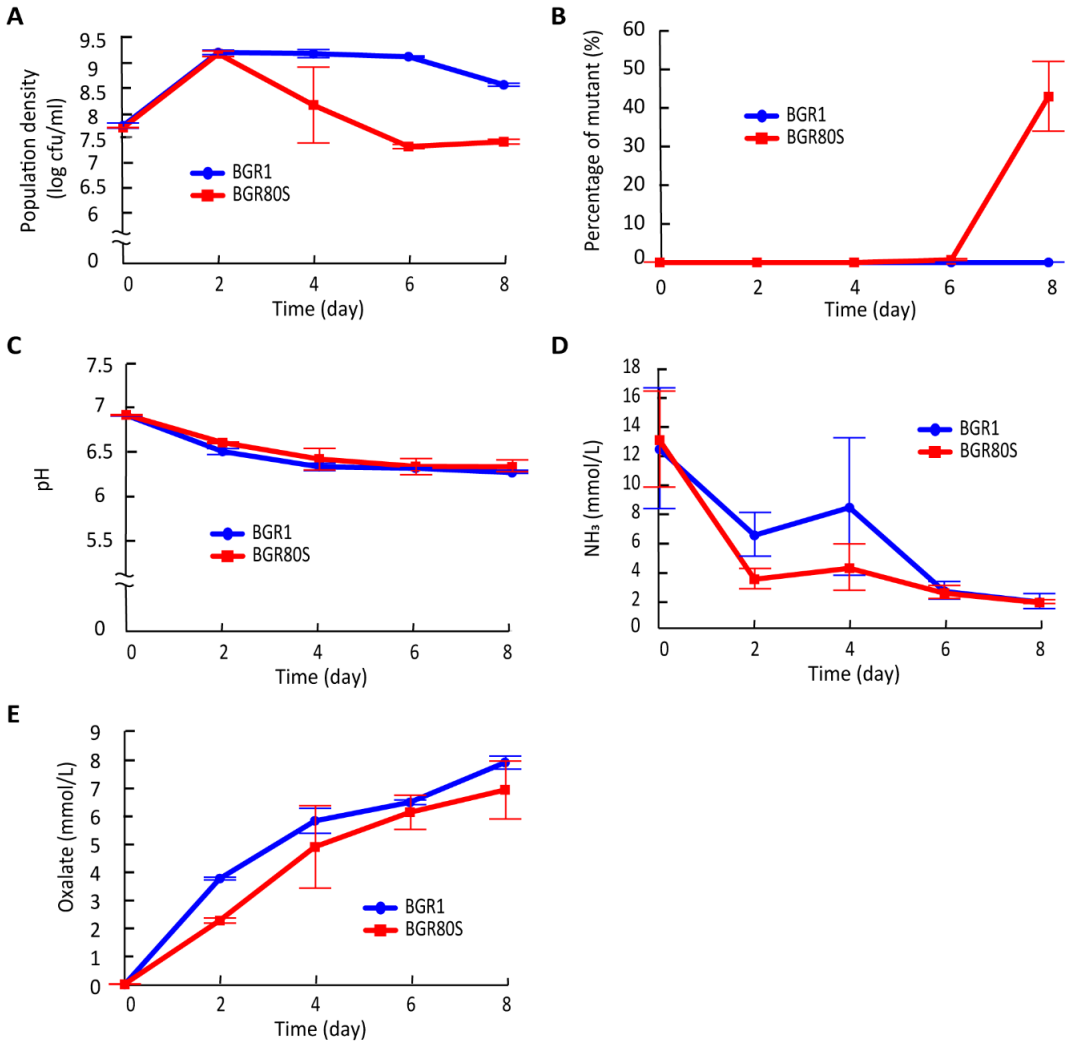
A
Population density (log cfu/ml)
Time (day)
BGR1
BGR80S
B
Percentage of mutant (%)
Time (day)
BGR1
BGR80S
C
pH
Time (day)
BGR1
BGR80S
D
NH₃ (mmol/L)
Time (day)
BGR1
BGR80S
E
Oxalate (mmol/L)
Time (day)
BGR1
BGR80S

Figure 12. Appearance of spontaneous mutant in BGR80S during growth in M9 minimal medium supplementing 0.4% glucose. (A) Cell viability, (B) the occurrence rate of spontaneous mutant, (C) the external pH, (D) ammonia and (E) oxalate production of the BGR1 and BGR80S were monitored at 0, 2, 4, 6, and 8 days after subculture. Data represent the mean ± SE of triplicates.

DISCUSSION

The genetic diversity of *B. glumae* strains, which are widely distributed in various niches, has been analyzed in many studies (Francis et al., 2013; Lee et al., 2016; Hussain et al., 2020; Choi et al., 2021; Cui et al., 2021). The clinical isolate AU6208 was reported to be more virulent on rice than the rice-pathogenic strains BGR1 and LMG 2196; however, nucleotide sequences showed 99.4% identity between the human- and plant-pathogenic strains (Cui et al., 2021). There was no significant difference in pathogenicity between Korean *B. glumae* isolates, despite the genetic diversity revealed by Tnp-PCR genomic fingerprinting (Choi et al., 2021). Likewise, no differences in pathogenicity were observed among the *B. glumae* isolates in this study, even though there were significant differences in genome structure, such as chromosomal merging.

It is increasingly recognized that, in addition to single-nucleotide changes, structural variations such as large genomic rearrangements can contribute to the evolution of an organism (Yeaman, 2013; Periwal and Scaria, 2015). Chromosomal rearrangements can disrupt an existing gene and create a new gene or chimeric gene product through gene fusions (Periwal and Scaria, 2015). In bacterial genomes, chromosomal rearrangements can affect gene expression by altering gene copy numbers, by changing the distance of a gene from the origin of chromosome replication (Rebollo et al., 1988). In this study, we aim to understand the genomic features of *B. glumae* isolates from various ecological niches and the effect of genomic differences on the physiology of *B. glumae*. By the results of analyzing and comparing the sequence and genome structures of the entire *B. glumae*

isolates, BGR76S, BGR22S, BGR28S, and BGR86S were in the same phylogenetic cluster as BGR80S and BGR80S, but their genome structure was completely different (Figure 1, 3). The appearance of spontaneous mutants in BGR80S and BGR81S under nutrient stress was not observed in others of the same cluster. From the results of this experiment, the occurrence frequency of spontaneous mutants seems to be more related to the genome structure than the sequence. The genomic structural variations provide deeper insight into the bacterial genome arrangement with much higher resolution (Periwal and Scaria, 2015).

Acquired kanamycin resistance can be transferred from donors to recipients by horizontal gene transfer (Leungtongkam et al., 2018). The *aphA* gene inserted into BGR57S, BGR59S, BGR68S, BGR73S, and BGR82S might have been introduced into *B. glumae* cells by horizontal gene transfer of plasmid such as pSCR001. pSCR001 carries Omegon-Km originating from pJFF350 (Fellay et al., 1987; Fellay et al., 1989; Giddens et al., 2007).

Naturally occurring *Vibrio cholera* strains with a single chromosome (in the form of merged chromosomes) have also been reported (Xie et al., 2017; Yamamoto et al., 2018). In *V. cholerae* strains NSCV1 and NSCV2, fusion junctions of chromosomes 1 and 2 contained more prophages, IS elements, repeats, and rearrangements compared to the prototypical two-chromosome *V. cholerae* genomes (Xie et al., 2017), but with no insertion of a foreign DNA fragment (unlike BGR80S and BGR81S). Similar to the virulence of the *V. cholerae* strains NSCV1 and NSCV2 seen in patients (Xie et al., 2017), BGR80S and BGR81S were associated with panicle blight symptoms in rice, because they still possessed virulence and toxoflavin genes (Figures 6, 7). Previous studies conducted on *V. cholerae* showed that homologous recombination in IS elements or recombination of *dif* sites, or

mutations of *crtS* (Chr2 replication triggering site) could cause chromosomal fusions (Xie et al., 2017). However, a more in-depth analysis is needed to determine whether these mechanisms are also the case in *B. glumae*. In addition, since two replication origins were identified on the fused chromosomes of BGR80S and BGR81S (Figure 4), similar to *V. cholerae* NSCV1 and NSCV2 (Xie et al., 2017), it is worth exploring whether they are involved in replication, as well as how the chromosomal merging is maintained and under what conditions it reverts to two separate chromosomes.

B. glumae utilizes the amino acids in LB medium as its carbon source, but most amino acids are depleted during the stationary phase (Goo et al., 2012; Marunga et al., 2021). Heterogeneity is typically observed in liquid medium batch cultures when nutrient depletion starts, and it increases when there is environmental stress, such as nutrient depletion or metabolic stress (Gasperotti et al., 2020). Appearance of heterogenetic variants is a putative adaptive response to adverse environmental conditions within an aging culture (Ryall et al., 2012). Although the occurrence of bacterial variants during batch cultures is common, the ideal mutations for survival are unknown. For *B. glumae* isolates, *qsmR* mutants are common for fitness benefits, and show varying occurrence frequencies depending on the genomic traits of the strain. However, the molecular mechanisms and associated genomic structures involved in inducing *qsmR* mutation are unknown. We previously reported occurrence of *qsmR* mutation under metabolic stress (Goo et al., 2017), however it is not known whether appearance of *qsmR* mutant is a common phenomenon in *B. glumae* under physiological stress. Once the mutant is isolated, it cannot survive due to the alkaline extracellular pH resulting from its inability to biosynthesize oxalate in a QS-

dependent manner as observed previously, since *B. glumae* is not viable above pH 8.5 (Goo et al., 2017; Goo et al., 2012).

Another question is whether the *B. glumae qsmR* mutants are cheaters that do not produce oxalate to benefit the population. Social cheaters emerge in populations growing in media requiring QS-regulated public goods, which increases the cost of cooperation (Sandoz et al., 2007; Dandekar et al., 2012). Based on two lines of evidence, the *qsmR* mutants isolated in this study are likely not cheaters. First, upon addition of casamino acids to the batch culture, a more significant amount of ammonia was released than in the plain LB, which increased the demand for oxalate (Figure 11). However, the *qsmR* mutant did not appear with daily addition of casamino acids. Second, the *qsmR* mutant appeared in M9 minimal medium, which scarcely requires oxalate (Figures 12). Therefore, the *qsmR* mutants isolated during batch culture might have undergone adaptation in a nutrient-depleted state.

Bacterial cooperative behaviors may conflict with individual interests (Diggle et al., 2007; Sandoz et al., 2007). Our study suggests that genome structure is correlated with adaptation to nutrient stress conditions and the emergence of QS-dependent gene regulation defects, which provide increased fitness benefits in *B. glumae*. However, in the previous studies on *Pseudomonas aeruginosa*, mutations in recognizing QS signals were commonly observed (Diggle et al., 2007), whereas in this study on *B. glumae*, mutations were observed in *qsmR*. Accordingly, further researches are needed to confirm the reason for these differences. The changing nutritional environment during the post-stationary phase is more akin to what bacteria experience in natural environments, where cells spend most of their

time under starvation and stress conditions. Our experiment provides insight into how genomic structural variations influence adaptive evolution, revealing evolutionary changes in an organism that make it compatible with its habitat.

LITERATURE CITED

Achtman, M., and Wagner, M. (2008) Microbial diversity and the genetic nature of microbial species. *Nat. Rev. Microbiol.* 6, 431-440. doi:10.1038/nrmicro1872

Aggeli, D., Li, Y., and Sherlock, G. (2021) Changes in the distribution of fitness effects and adaptive mutational spectra following a single first step towards adaptation. *Nat. Commun.* 12, 5193. doi:10.1038/s41467-021-25440-7

Chin, C.S., Alexander, D.H., Marks, P., Klammer, A.A., Drake, J., Heiner, C., et al. (2013) Nonhybrid, finished microbial genome assemblies from long-read SMRT sequencing data. *Nat. Methods.* 10, 563-569. doi: 10.1038/nmeth.2474

Choi, O., Kim, S., Kang, B., Lee, Y., Bae, J., and Kim, J. (2021) Genetic diversity and distribution of Korean isolates of *Burkholderia glumae. Plant Dis.* 105, 1398-1407. doi:10.1094/PDIS-08-20-1795-RE

Cui, Z., Wang, S., Kakar, K.U., Xie, G., Li, B., and Chen, G. (2021) Genome sequence and adaptation analysis of the human and rice pathogenic strain *Burkholderia glumae* AU6208. *Pathogens.* 10, 87. doi:10.3390/pathogens10020087

Dandekar, A.A., Chugani, S., and Greenberg, E.P. (2012) Bacterial quorum sensing and metabolic incentives to cooperate. *Science* 338, 264-266. doi:10.1126/science.1227289

Diggle, S. P., Griffin, A. S., Campbell, G. S., & West, S. A. (2007). Cooperation and conflict in quorum-sensing bacterial populations. *Nature*, 450(7168), 411-414.

Francis, F., Kim, J., Ramaraj, T., Farmer, A., Rush, M.C., and Ham, J.H. (2013) Comparative genomic analysis of two *Burkholderia glumae* strains from different geographic origins reveals a high degree of plasticity in genome structure associated with genomic islands. *Mol. Genet. Genomics.* 288, 195-203. doi:10.1007/s00438-013-0744-x

Fellay, R., Frey, J., and Krisch, H. (1987) Interposon mutagenesis of soil and water bacteria: a family of DNA fragments designed for in vitro insertional mutagenesis of gram-negative bacteria. *Gene* 52, 147-154. doi:10.1016/0378-1119(87)90041-2

Fellay, R., Krisch, H.M., Prentki, P., and Frey, J. (1989) Omegon-Km: a transposable element designed for in vivo insertional mutagenesis and cloning of genes in gram-negative bacteria. *Gene* 76, 215-226. doi:10.1016/0378-1119(89)90162-5

Gasperotti, A., Brameyer, S., Fabiani, F., and Jung, K. (2020) Phenotypic heterogeneity of microbial populations under nutrient limitation. *Curr. Opin. Biotechnol.* 62, 160-167. doi:10.1016/j.copbio.2019.09.016

Giddens, S.R., Jackson, R.W., Moon, C.D., Jacobs, M.A., Zhang, X.X., Gehrig, S.M., et al. (2007) Mutational activation of niche-specific genes provides insight into regulatory networks and bacterial function in a complex environment. *Proc. Natl. Acad. Sci. U.S.A.* 104, 18247-18252. doi:10.1073/pnas.0706739104

Goo, E. and Hwang, I. (2021) Essential roles of Lon protease in the morpho-physiological traits of the rice pathogen *Burkholderia glumae*. *PLoS One*. 16, e0257257. doi:10.1371/journal.pone.0257257

Goo, E., Kang, Y., Lim, J.Y., Ham, H., and Hwang, I. (2017) Lethal consequences of overcoming metabolic restrictions imposed on a cooperative bacterial population. *mBio* 8, e00042-17. doi:10.1128/mBio.00042-17

Goo, E., Majerczyk, C.D., An, J.H., Chandler, J.R., Seo, Y.S., Ham, H., et al. (2012) Bacterial quorum sensing, cooperativity, and anticipation of stationary-phase stress. *Proc. Natl. Acad. Sci. U.S.A.* 109, 19775-19780. doi:10.1073/pnas.1218092109

Helsen, J., Voordeckers, K., Vanderwaeren, L., Santermans, T., Tsontaki, M.,Verstrepen, K.J., et al. (2020) Gene loss predictably drives evolutionary adaptation. *Mol. Biol. Evol.* 37, 2989-3002. doi:10.1093/molbev/msaa172

Hussain, A., Shahbaz, M., Tariq, M., Ibrahim, M., Hong, X., Naeem, F., et al. (2020) Genome re-sequence and analysis of *Burkholderia glumae* strain AU6208 and evidence of toxoflavin: A potential bacterial toxin. *Comput. Biol. Chem.* 86, 107245. doi:10.1016/j.compbiolchem.2020.107245

Jeong, Y., Kim, J., Kim, S., Kang, Y., Nagamatsu, T., and Hwang, I. (2003) Toxoflavin produced by *Burkholderia glumae* causing rice grain rot is responsible for inducing bacterial wilt in many field crops. *Plant Dis*. 87, 890. doi: 10.1094/PDIS.2003.87.8.890

Kim, J., Kim, J.G., Kang, Y., Jang, J.Y., Jog, G.J., Lim, J.Y., et al. (2004) Quorum sensing and the LysR-type transcriptional activator ToxR regulate toxoflavin biosynthesis and transport in *Burkholderia glumae*. *Mol. Microbiol.* 54, 921–934. doi:10.1111/j.1365-2958.2004.04338.x

Kim, J., Kang, Y., Choi, O., Jeong, Y., Jeong, J.E., Lim, J.Y., et al. (2007) Regulation of polar flagellum genes is mediated by quorum sensing and FlhDC in *Burkholderia glumae. Mol. Microbiol.* 64, 165–179. doi:10.1111/j.1365-2958.2007.05646.x

Lee, H.H., Park, J., Kim, J., Park, I., and Seo, Y.S. (2016) Understanding the direction of evolution in *Burkholderia glumae* through comparative genomics. *Curr. Genet.* 62, 115-123. doi:10.1007/s00294-015-0523-9

Leungtongkam, U., Thummeepak, P., Tasanapak, K., and Sitthisak, S. (2018) Acquisition and transfer of antibiotic resistance genes in association with conjugative plasmid or class 1 integrons of *Acinetobacter baumannii. PLoS One*. 13, e0208468. doi:10.1371/journal.pone.0208468

Lim, J., Lee, T.H., Nahm, B.H., Choi, Y.D., Kim, M., and Hwang, I. (2009) Complete genome sequence of *Burkholderia glumae* BGR1. *J. Bacteriol.* 191, 3758-3759. doi:10.1128/JB.00349-09

Marunga, J., Goo, E., Kang, Y., and Hwang, I. (2021) Identification of a genetically linked but functionally independent two-component system important for cell division of the rice pathogen *Burkholderia glumae*. *Front. Microbiol.* 12, 700333.

doi:10.3389/fmicb.2021.700333

Periwal, V., and Scaria, V. (2015) Insights into structural variations and genome rearrangements in prokaryotic genomes. *Bioinformatics*. 31, 1-9. doi:10.1093/bioinformatics/btu600

Ratib, N.R., Seidl, F., Ehrenreich, I.M., and Finkel, S.E. (2021) Evolution in long-term stationary-phase batch culture: emergence of divergent *Escherichia coli* lineages over 1,200 days. *mBio* 12, e03337-20. doi:10.1128/mBio.03337-20

Rebollo, J.E., François, V., and Louarn, J.M. (1988) Detection and possible role of two large nondivisible zones on the *Escherichia coli* chromosome. *Proc. Natl. Acad. Sci. U.S.A*. 85, 9391-9395. doi:10.1073/pnas.85.24.9391

Ryall, B., Eydallin, G., and Ferenci, T. (2012) Culture history and population heterogeneity as determinants of bacterial adaptation: the adaptomics of a single environmental transition. *Microbiol. Mol. Biol. Rev*. 76, 597-625. doi:10.1128/MMBR.05028-11

Sambrook, J., Fritsch, E.F., and Maniatis, T. (1989). Molecular cloning: a laboratory manual. New York: Cold Spring Harbor Laboratory Press.

Sandoz, K.M., Mitzimberg, S.M., and Schuster, M. (2007) Social cheating in *Pseudomonas aeruginosa* quorum sensing. *Proc. Natl. Acad. Sci. U.S.A.* 104, 15876-15881. doi:10.1073/pnas.0705653104

Weinberg, J.B., Alexander, B.D., Majure, J.M., Williams, L.W., Kim, J.Y., Vandamme, P., et al. (2007) *Burkholderia glumae* infection in an infant with chronic

granulomatous disease. *J. Clin. Microbiol*. 45, 662-665. doi:10.1128/JCM.02058-06

Xie, G., Johnson, S.L., Davenport, K.W., Rajavel, M., Waldminghaus, T., Detter, J.C., et al. (2017) Exception to the rule: genomic characterization of naturally occurring unusual *Vibrio cholerae* strains with a single chromosome. *Int. J. Genomics* 2017, 8724304. doi:10.1155/2017/8724304

Yamamoto, S., Lee, K.I., Morita, M., Arakawa, E., Izumiya, H., and Ohnishi, M. (2018) Single circular chromosome identified from the genome sequence of the *Vibrio cholerae* O1 bv. El Tor Ogawa Strain V060002. *Genome Announc*. 6, e00564-18. doi:10.1128/genomeA.00564-18

Yeaman, S. (2013) Genomic rearrangements and the evolution of clusters of locally adaptive loci. *Proc. Natl. Acad. Sci. U.S.A*. 110, E1743-E1751. doi:10.1073/pnas.1219381110

Zhao, Y., Wu, J., Yang, J., Sun, S., Xiao, J., and Yu, J. (2012) PGAP: pan-genomes analysis pipeline. *Bioinformatics* 28, 416-418. doi:10.1093/bioinformatics/btr655

세균벼알마름병균 (*Burkholderia glumae*)에서 유전체 구조와 양분 스트레스가 정족수 감지 기반 유전자 조절 돌연변이의 발생에 미치는 영향

강 민 희

초 록

세균은 척박한 환경에 적응하기 위하여 그들의 유전적, 생리적 특성들을 바꾼다. 세균벼알마름병원균 (*Burkholderia glumae*)은 넓은 기주 범위를 가지는 식물병원균으로 세균성 시들음병이나 세균벼알마름병을 일으킨다. 세균벼알마름병원균은 생태학적 환경에 대한 높은 다양성과 적응성을 보인다. 이번 연구에서는 세균벼알마름병균에서 유전적 다양성과 변화하는 환경에 적응하는 능력이 연관이 있는지를 알아보기 위하여 서로 다른 숙주와 지역에서 분리한 44개 분리균들의 전체 유전체를 분석하였다. 전체 유전체의 계통학적 분석을 바탕으로 전체 분리균은 2개의 분할과 6개의 군집으로 나누어 졌다. 두 개의 염색체가 하나로 합쳐진 형태를 가진 BGR80S와 BGR81S를 제외한 모든 분

리균들은 2개의 염색체를 소유한 것으로 나타났다. 각각의 유전체 구조를 비교 기준이 되는 균주인 BGR1과 비교하였을 때, 염색체 1번 또는 2번에서 역위, 결실 및 재배열 등이 관찰되었다. 또한 BGR1과 비교하였을 때 유전체 구조에 차이를 보였던 BGR80S, BGR15S, BGR21S 균주를 Luria-Bertani (LB) 배지에서 키웠을 때, *qsmR* 유전자 (quorum-sensing master regulator를 암호화하는 유전자)가 제 기능을 하지 못하는 자연 돌연변이가 발생하였다. BGR15S와 BGR21S에서는 계대배양 6일째부터 돌연변이가 관찰되기 시작하여 8일째 돌연변이의 비율이 약 40%에 달하였다. BGR80S에서는 계대배양 2일째부터 돌연변이가 관찰되기 시작하며 8일째 돌연변이의 비율이 약 80%에 달하였다. BGR1과 BGR13S에서는 관측한 기간 동안 측정 가능한 빈도로 돌연변이가 검출되지 않았다. 이러한 *qsmR* 돌연변이는 정상 균주와 함께 배양하였을 때 정상 균주에 비하여 우세하게 자랐다. 또한 BGR80S의 회분배양에서 포도당이나 카사미노산을 매일 추가하면 돌연변이의 출현이 지연되고 그 빈도가 감소하였다. 이러한 결과는 *qsmR* 자연 돌연변이가 유전체 구조 및 양분 스트레스와 연관성을 가진다는 것을 보여준다.

주요어: 세균벼알마름병균, 유전체 다양성, QsmR 돌연변이, 적응

학번: 2015-23124